Cadherin-26 drives macrophage alternative activation via suppressing STUB1-mediated IL-4Rα ubiquitination in asthma

Gongqi Chen[1,2,3], Shengchong Chen[1,2,3], Chunli Huang[1,2,3], Wei Gu[1,2,3], Huiru Jie[1,2,3], Lu Zhao[1,2,3], Weiqiang Kong[1,2,3], Jiali Gao[1,2,3], Yuchen Feng[1,2,3], Lingling Yi[1,2,3], Guohua Zhen[1, 2,3]

[1]Division of Respiratory and Critical Care Medicine, Department of Internal Medicine, Tongji Hospital, Tongji Medical College, Huazhong University of Science and Technology, Wuhan 430030, China; [2]Key Laboratory of Respiratory Diseases, National Health Commission of the People's Republic of China; [3] National Clinical Research Center for Respiratory Diseases, Wuhan, China

Correspondence to: Guohua Zhen, Division of Respiratory and Critical Care Medicine, Tongji Hospital, Wuhan, China 430030; Email: ghzhen@tjh.tjmu.edu.cn

This work is supported by National Natural Science Foundation of China (grant 82170036), Key Research and Development Program of Hubei Province (grant 2024BCB280), Innovation and Translation Project of Tongji Hospital (grant 2023CXZH006), Natural Science Foundation of Hubei Province (2024AFB622), Research Foundation of Tongji Hospital (2023B06)

Rationale： IL-4 receptor (IL-4R)-mediated alternative activation of macrophage drives type 2 airway inflammation. Cadherin-26 (CDH26) upregulates epithelial type II IL-4R signaling in asthma. However, whether CDH26 contributes to type I IL-4R-mediated macrophage activation and the mechanism by which CDH26 upregulates IL-4R expression remains unknown.

Objectives: To investigate whether CDH26 promotes macrophage alternative activation via suppressing IL-4Rα ubiquitination-proteasomal degradation.

Methods: CDH26 expression in bronchoalveolar lavage cells of asthma patients was examined using quantitative PCR and immunostaining. Airway inflammation and macrophage activation were assessed in ovalbumin-sensitized and challenged macrophage-specific *Cdh26*-deficient mice. Mechanistic experiments included IL-4Rα degradation and ubiquitination assay, CDH26 co-immunoprecipitation and mass spectrometry analysis. *Cdh26* siRNA encapsulated lipid nanoparticles were used to treat the mouse model.

Measurements and Results: CDH26 expression was enhanced in bronchoalveolar lavage cells from patients with eosinophilic asthma and was localized to lung macrophages. Airway eosinophilia, mucus overproduction and macrophage alternative activation were significantly suppressed in ovalbumin-challenged macrophage-specific *Cdh26*-deficient mice compared to control mice. *Cdh26* deficiency inhibits IL-4Rα expression and STAT6 phosphorylation in macrophages in vitro. Furthermore, CDH26 knockdown enhances whereas CDH26 overexpression suppresses IL-4Rα ubiquitination and proteasomal degradation. Mechanistically, CDH26 directly interacts

with STUB1 and suppresses the binding of STUB1 to IL-4Rα and subsequent ubiquitination-proteasomal degradation. *Cdh26* siRNA encapsulated lipid nanoparticles markedly alleviate airway inflammation, mucus overproduction and macrophage alternative activation in the mouse model.

Conclusions: CDH26 interacts with STUB1 and suppresses STUB1-mediated IL-4Rα ubiquitination-proteasomal degradation, thereby amplifying IL-4R signaling in macrophages in asthma. CDH26 is a potential therapeutic target for asthma.

Keywords: asthma; cadherin-26; IL-4 receptor; ubiquitination-proteasomal degradation; macrophage alternative activation.

At a glance commentary

Scientific knowledge on the subject: IL-4R signaling drives macrophage alternative activation, mucous cell metaplasia, and type 2 airway inflammation in asthma, but the regulatory mechanism underlying IL-4R expression remains unclear.

What this study adds to the field: CDH26 expression is enhanced in lung macrophages from patients with eosinophilic asthma. Macrophage-specific *Cdh26* deficiency suppresses macrophage alternative activation and airway eosinophilia in a mouse model of allergic airway inflammation. CDH26 directly interacts with STUB1 and suppresses STUB1-mediated IL-4Rα ubiquitination-proteasomal degradation, resulting in sustained activation of IL-4R signaling. Lipid nanoparticles encapsulating *Cdh26* siRNA effectively alleviate airway eosinophilia and mucus overproduction in the mouse model.

Introduction:

Asthma is a chronic airway disease that characterized by airway inflammation, mucus overproduction, airway remodeling, and airway hyperresponsiveness (1). Asthma affects approximately 358 million people worldwide and is among the top five respiratory diseases posing a threat to global health (2). Severe asthma imposes significant burdens on individuals and society, with the potential for fatal outcomes (3). Eosinophilic airway inflammation driven by type 2 immune response is commonly observed in severe asthma patients (4).

Macrophages play an important role in environmental allergen-induced airway inflammation in asthma (5). Macrophages exhibit different activation states in response to various stimuli (6). When activated by microbes-induced factors such as interferon-γ and reactive oxygen species, macrophages switch to a pro-inflammatory state named as classical activation (M1 macrophages) and eliminate engulfed microbes (7). On the other hand, when activated by allergen-induced type 2 cytokines including IL-4 and IL-13, macrophages are alternatively activated (M2 macrophages) to promote tissue repair, remodeling, and wound healing (8). Macrophage alternative activation is involved in the development of allergic diseases including asthma (9). Alternatively activated macrophages release high levels of IL-13 and chemokines including CCL17, CCL18, CCL22, and CCL24, which activate Th2 cells and promote eosinophilic inflammation (10).

The IL-4R-STAT6 signaling pathway plays a crucial role in the alternative activation of macrophages (11). There are two types of IL-4R (12). Type I IL-4R

consists of IL-4Rα and IL-2Rγ (γc) subunits and is expressed in hematopoietic cells including lymphocytes and macrophages (13). Type II IL-4R, composed of IL-4Rα and IL-13Rα1 subunits, is present in hematopoietic and non-hematopoietic cells including airway epithelial cells and smooth muscle cells (14). Type I IL-4R specifically binds to IL-4, leading to downstream JAK1-STAT6 activation and macrophages alternative activation (15). Meanwhile, the occupied IL-4R is degraded to terminate and prevent sustained activation of IL-4R signaling. There are several mechanisms underlying IL-4R degradation including endocytosis and ubiquitin-proteasome system(16-18). Wei and colleagues demonstrated that STIP1 homology and U-box-containing protein 1 (STUB1), an E3 ligase, interacts with IL-4Rα, a subunit shared by type I and type II IL-4R, to lead to its ubiquitination and proteasomal degradation (17).

Cadherin family members including cadherin-1 play important roles in maintaining the adhesive connections between airway epithelial cells as well as regulating epithelial cell proliferation and differentiation (19). CDH26, a non-classical member of cadherin family, contributes to apicobasal polarization of airway epithelial cells (20). CDH26 has long been associated to type 2 inflammation-related diseases including asthma, helminth infection, eosinophilic gastritis, and esophagitis (21-24), but the precise role of CDH26 in these diseases is unclear. We recently reported that CDH26 promotes airway eosinophilia and mucus overproduction via upregulating epithelial type II IL-4R signaling (25). However, whether CDH26 contributes to type I IL-4R-mediated macrophage activation and the mechanism by which CDH26 upregulates IL-4R expression remains unknown.

In this study, we observed elevated CDH26 expression in lung macrophages from patients with eosinophilic asthma. Macrophage-specific *Cdh26* deficiency significantly suppressed macrophage alternative activation, airway eosinophilia, and mucus overproduction in a mouse model of allergic airway inflammation. CDH26 knockdown or overexpression accelerated or inhibited IL-4Rα proteasomal degradation in vitro, respectively. Mechanistically, CDH26 interacts with STUB1 to suppress its binding to IL-4Rα, thus inhibiting IL-4Rα ubiquitination and degradation. Intriguingly, *Cdh26* siRNA encapsulated lipid nanoparticles effectively alleviated airway eosinophilia and mucus overproduction in the mouse model.

Materials and methods:

For additional information on the materials and methods used in this study, please refer to the online supplementary materials.

Subjects

We recruited 17 control subjects, 25 eosinophilic asthma patients (sputum eosinophils > 3%), and 7 non-eosinophilic asthma patients (sputum eosinophil ≤ 3%) (26). All participants provided written informed consent, and the study was approved by the ethics committee of Tongji Hospital, Tongji Medical College, Huazhong University of Science and Technology.

Murine model of allergic airway inflammation

Cdh26$^{fl/fl}$*Lyz2Cre* mice on a C57BL/6N background were generated and provided by GemPharmatech (Nanjing, China). Exon 4 of *Cdh26* gene was deleted in *Cdh26*$^{fl/fl}$*Lyz2Cre* mice. All experimental procedures were approved by the Animal Care

and Use Committee of Tongji Hospital, Tongji Medical College, Huazhong University of Science and Technology.

Statistical analysis

Data analysis was performed using Prism version 8 (GraphPad Software). For normally distributed data, we calculated the means ± standard deviation (SD) and performed Student's *t* test or one-way ANOVA followed by Tukey's multiple comparison test to compare across groups. For non-normally distributed data, we calculated medians with interquartile ranges and performed Mann-Whitney test. Spearman's correlation coefficient was used to assess correlation. Statistical significance was defined as $p < 0.05$.

Results:

1. CDH26 expression is upregulated in lung macrophages from eosinophilic asthma patients.

We initially examined the expression of CDH26 in BAL cells from our cohort of mild-moderate asthma (n=32) and control subjects (n=17). The transcript levels of *CDH26* in BAL cells were determined using quantitative PCR. *CDH26* transcript levels were significantly higher in BAL cells from asthma patients compared to control subjects (Figure 1A). We further classified asthma patients as eosinophilic asthma (n=25, sputum eosinophils > 3%) and non-eosinophilic asthma (n=7, sputum eosinophils ≤ 3%) (26). *CDH26* transcript levels were significantly higher in BAL cells from eosinophilic asthma patients compared to control subjects, but no significant difference was observed between non-eosinophilic asthma patients and control subjects

(Figure 1B). Moreover, *CDH26* transcript levels in BAL cells of asthma patients showed a strong correlation with fractional exhaled nitric oxide (FeNO) (r_s=0.6038, p=0.0004), an indicator of airway eosinophilia (Figure 1C). *CDH26* transcript levels were also correlated with sputum eosinophil percentages and serum IgE (Figures 1D, E1E). Additionally, the transcript levels of *CDH26*, *CD206*, *FIZZ1* and *CCL17*, molecular markers for macrophage alternative activation, were all significantly increased in sputum cells from asthma patients compared to control subjects (Figures E1A-E1D).

We next examined the expression of CDH26 in BAL cells using immunohistochemistry and found a significant increase in the number of CDH26-expressing cells in BAL cells from asthma patients (n=4) compared to control subjects (n=4) (Figures 1E-1F). Immunofluorescence staining of BAL cells with CDH26 and CD68, a marker for macrophages, revealed that CDH26 was localized to enlarged foamy CD68-expressing cells, and the fluorescent intensity of CDH26 relative to CD68 was markedly increased in asthma patients (Figures 1H-1I). Of note, the $CDH26^{+}CD68^{+}$ cells from asthma patients exhibited an enlarged, foamy, and granular morphology, which was previously reported to be associated with alternative activation of macrophages (27). This suggests that CDH26 is expressed in activated macrophages and its expression is upregulated in asthma. Taking advantage of open-access gene expression datasets of sputum cells or BAL cells from asthma patients, we analyzed a microarray dataset (GSE76262) using sputum cells from mild-moderate asthma (n=25) and severe asthma (n=49), and found that the expression levels of *CDH26* were

significantly higher in the sputum cells from patients with severe asthma compared to mild-moderate asthma (28). This suggests that *CDH26* expression is even higher in severe asthma. Moreover, there is a positive correlation between the expression levels of *CDH26* and *CCL17* in asthma patients (Figures E1F-1G). We further analyzed an RNA-seq dataset (GSE2125) using alveolar macrophages isolated from control subjects and asthma patients, and found that the expression levels of *CDH26* were significantly higher in macrophages from asthma patients (n=15) compared to control subjects (n=15) (Figure 1J) (29). This supports our findings that CDH26 is upregulated in lung macrophages in asthma. Together, our data suggest that CDH26 expression is upregulated in lung macrophages of eosinophilic asthma or severe asthma.

2. Macrophage-specific *Cdh26* deficiency alleviates airway eosinophilia and mucus overproduction in a mouse model of allergic airway inflammation.

We next examined the expression of Cdh26 in BAL cells from wild type (WT) mice and observed enlarged, foamy $Cdh26^{+}Cd68^{+}$ cells in in ovalbumin (OVA)-sensitized and challenged WT mice (Figures 2A). The fluorescent intensity of Cdh26 relative to Cd68 were increased in OVA challenged WT mice (Figures 2B). We observed that global *Cdh26* deficiency significantly inhibited airway eosinophilia and the expression of molecular makers for macrophage alternative activation in the mouse model (Figures E2-E3). We further utilized macrophage-specific *Cdh26*-deficient mice generated by crossing *Lyz2Cre* mice and $Cdh26^{fl/fl}$ mice (Figures E4A-E4C, 2C). H&E staining and morphological inflammatory scoring revealed that OVA-induced peribronchial inflammation was alleviated in $Cdh26^{fl/fl}Lyz2Cre$ mice compared to

Cdh26$^{fl/fl}$ mice (Figures 2D-2E). OVA challenge increased the number of eosinophils in BAL of *Cdh26*$^{fl/fl}$ mice, but this increase was significantly reduced in *Cdh26*$^{fl/fl}$*Lyz2Cre* mice (Figure 2G). The number of PAS-staining-positive mucous cells and the airway resistance to methacholine were increased in OVA-challenged compared to saline-challenged *Cdh26*$^{fl/fl}$ mice. However, the mucous cell metaplasia and airway hyperresponsiveness were significantly attenuated in *Cdh26*$^{fl/fl}$*Lyz2Cre* mice compared to *Cdh26*$^{fl/fl}$ mice (Figures 2D, 2F, 2H). In addition, Masson trichrome staining revealed that collagen area was significantly reduced in *Cdh26*$^{fl/fl}$*Lyz2Cre* mice (Figures E5A-E5B). Our findings suggest that macrophage *Cdh26* is required for eosinophilic airway inflammation, mucus overproduction, and airway hyperresponsiveness in asthma.

3. Cdh26 is required for macrophage alternative activation.

We further evaluated the effect of macrophage-specific *Cdh26* deficiency on macrophage alternative activation. Immunofluorescence staining for Cd68 and Cd206, a marker for M2 macrophage, were performed using BAL cells from mice. The number of Cd68^{+}Cd206^{+} BAL cells was increased in OVA-challenged *Cdh26*$^{fl/fl}$ mice, while this increase was suppressed in *Cdh26*$^{fl/fl}$*Lyz2Cre* mice (Figures 3A-3B). We also used flow cytometry to evaluate macrophage alternative activation in lung tissue. Defining Cd45^{+}Cd11b^{+}Cd206^{+} cells as M2 macrophages (Figure E4D), we observed a significant reduction in the number of Cd45^{+}Cd11b^{+}Cd206^{+} cells in lung tissue of OVA-challenged *Cdh26*$^{fl/fl}$*Lyz2Cre* mice compared to *Cdh26*$^{fl/fl}$ mice (Figures 3C-3D). Consistently, western blotting showed reduced expression of M2 markers Arg1 and Cd206 in lung tissue of OVA-challenged *Cdh26*$^{fl/fl}$*Lyz2Cre* mice (Figures 3E-3G). The transcript levels

of *Cd206* and *Ym1* were also decreased in lung tissue of *Cdh26*$^{fl/fl}$*Lyz2Cre* mice (Figures 3H-3K). M2 macrophages can recruit Th2 cells and promote eosinophilic airway inflammation by secreting CCL17 and CCL22 (30). We found a reduction in transcript and protein levels of Ccl17 and Ccl22 in lung tissue and BALF from OVA-challenged *Cdh26*$^{fl/fl}$*Lyz2Cre* mice, respectively (Figures 3L-3O).

In vitro, we stimulated mouse bone marrow-derived macrophages (BMDMs) and lung macrophages from WT mice with LPS and IL-4, respectively. The transcription levels of *Cdh26* were increased after IL-4 stimulation, but not altered after LPS stimulation (Figures E6A-E6F). Moreover, we stimulated WT BMDMs with IL-4 or IL-13 and found that only IL-4 enhanced the expression of *Cdh26* (Figures E6G-E4I). The expression of M2 markers in IL-4-stimulated BMDM derived from *Cdh26*$^{-/-}$ mice were significantly suppressed compared to IL-4-stimulated BMDMs from control mice (Figures E7). Similar results were observed in cultured mouse lung macrophages (Figures E8). Our data suggest that *Cdh26* is required for macrophage alternative activation.

4. *Cdh26* deficiency suppresses IL-4R expression and IL-4R-STAT6 signaling in macrophages.

Type I IL-4R consisting of IL-4Rα and IL-2Rγ (γc) subunits plays a central role in macrophage alternative activation (15). We examined the expression of CDH26 and IL-4Rα in BAL cells using immunofluorescence staining, and found that both CDH26 and IL-4Rα were localized in some CD206^{+} macrophages (Figure 4A), and the number of CDH26^{+}IL-4Rα^{+}CD206^{+} cells were markedly increased in asthma patients (n=4)

compared to control subjects (n=4) (Figure 4B). This suggests that CDH26 and IL-4Rα are co-expressed in alternatively activated macrophages in human asthma. Moreover, the transcription levels of *IL4RA* were increased in sputum cells of our mild-moderate asthma patients compared to control subjects (Figure 4C). Of note, analysis of the aforementioned dataset (GES76262) revealed that the expression levels of *IL4RA* in sputum cells were significantly higher in severe asthma compared to mild-moderate asthma (Figure 4D). These data suggest that IL-4Rα is upregulated in alternatively activated macrophages in asthma.

We next examined the transcript and protein levels of Il-4Rα in BMDMs from WT and *Cdh26*$^{-/-}$ mice. *Cdh26* deficiency suppressed the protein level of Il-4Rα whereas did not alter its transcription level, suggesting that Cdh26 may regulate Il-4Rα expression post-translationally (Figures 4E-4G). We further assessed the phosphorylation of STAT6 using western blotting and observed that *Cdh26* deficiency significantly inhibited Il-4-induced STAT6 phosphorylation in BMDMs (Figures 4H-4I). To further investigate the impact of *Cdh26* deficiency on Il-4Rα expression in M2 macrophages, we performed co-immunofluorescence staining of Il-4Rα and Cd206 in BAL cells from saline or OVA-challenged *Cdh26*$^{fl/fl}$*Lyz2Cre* and *Cdh26*$^{fl/fl}$ mice. OVA challenge increased the number of Il-4Rα^{+} and Il-4Rα^{+}Cd206^{+} cells in BAL cells from *Cdh26*$^{fl/fl}$ mice, while the number of Il-4Rα^{+} and Il-4Rα^{+}Cd206^{+} cells were decreased in OVA-challenged *Cdh26*$^{fl/fl}$*Lyz2Cre* mice (Figures 4J-4L). Similar results were observed in saline or Il-4-stimulated BMDMs derived from *Cdh26*$^{fl/fl}$ and *Cdh26*$^{fl/fl}$*Lyz2Cre* mice (Figures 4M-4O). Our data suggest that *Cdh26* deficiency

suppresses IL-4Rα expression and the IL-4R-STAT6 signaling pathway in macrophages.

5. CDH26 enhances IL-4Rα expression via inhibiting its ubiquitination and degradation.

We next used cycloheximide, an inhibitor of protein synthesis, to treat A549 cells which constitutively express IL-4Rα, and assessed the impact of CDH26 knockdown or overexpression on the degradation rate of IL-4Rα and IL-2Rγ. CDH26 knockdown significantly accelerated the degradation rate of IL-4Rα whereas did not alter the degradation rate of IL-2Rγ (Figures 5A-5C). Conversely, CDH26 overexpression significantly suppressed the degradation rate of IL-4Rα whereas did not alter the degradation rate of IL-2Rγ (Figures 5D-5F). This indicates that CDH26 suppresses IL-4Rα degradation.

Protein degradation pathways mainly include the ubiquitin-proteasome pathway and the lysosome pathway. To investigate the specific mechanism by which CDH26 suppresses IL-4Rα degradation, we used the proteasome pathway inhibitor MG132 and the lysosome pathway inhibitor chloroquine (CQ) to treat A549 cells transfected with CDH26 siRNA. We found that CDH26 knockdown decreased IL-4Rα protein level while MG132 restored the protein level of IL-4Rα. However, chloroquine did not affect IL-4Rα protein expression (Figures 5G-5J). These results suggest that CDH26 may inhibit IL-4Rα degradation through the ubiquitin-proteasome pathway. In support of this, we found that CDH26 overexpression significantly inhibited the ubiquitination level of IL-4Rα (Figures 5K). Together, our findings suggest that CDH26 enhances IL-4Rα expression via inhibiting its ubiquitination and degradation.

6. CDH26 interacts with STUB1 to restrain the binding of STUB1 with IL-4Rα.

To further explored the mechanism by which CDH26 inhibits IL-4Rα ubiquitination-proteasomal degradation, we transfected HEK-293T cells with CDH26-FLAG overexpression plasmid. Co-immunoprecipitation experiment using FLAG antibody and mass spectrometry analysis were performed to identify the proteins interacting with CDH26 (Figures 6A, E9A-E9B). A total of 423 proteins interacting with CDH26 were identified and they were intersected with the molecules involved in "Ubiquitin mediated proteolysis" pathway in KEGG database, resulting in the identification of four molecules: UBE3C, STUB1, CDC20, and UBE2G2 (Figures 6B-6C). A previous study demonstrated that STUB1 acts as an E3 ubiquitin ligase responsible for IL-4Rα ubiquitination and subsequent degradation (17).We found no significant difference in *STUB1* transcripts in airway brushing between asthma patients and control subjects, but *STUB1* transcripts were slightly decreased in BAL cells from asthma patients compared to control subjects (Figures 6D-6E). In addition, there was no difference in STUB1 transcript and protein levels in lung tissues between OVA-challenged $Cdh26^{fl/fl}$ and $Cdh26^{fl/fl}Lyz2Cre$ mice (Figures 6F-6H).

We further confirmed the interaction between CDH26 and STUB1 using protein immunoprecipitation experiments. Coimmunoprecipitation assay using STUB1 antibody to capture protein complexes in HEK-293T lysates showed that CDH26 coprecipitated with STUB1 (Figure 6I). In reciprocal experiments, overexpression of FLAG-tagged CDH26 ($CDH26^{FLAG}$) in HEK-293T cells resulted in the coprecipitation of STUB1 with the antibody against FLAG (Figure 6J). To explore the impact of the

CDH26-STUB1 interaction on the ubiquitination of IL-4Rα, we transfected HEK-293T cells with a plasmid overexpressing CDH26 and observed a significant inhibition of STUB1 levels binds to IL-4Rα, as well as a decrease in the ubiquitination level of IL-4Rα (Figure 6M). This suggests that CDH26 may competitively bind to STUB1, inhibiting the binding of STUB1 with IL-4Rα and its subsequent ubiquitination. In support of this, CDH26 knockdown significantly inhibited the elevation of IL-4Rα protein level induced by STUB1 knockdown (Figures 6K-6L).

Next, we attempted to determine the potential binding sites of CDH26 required for its interaction with STUB1. Using the predicted structures of CDH26 (uniProt ID: Q8IXH8) and STUB1 (uniProt ID: Q9UNE7) from the AlphaFold protein structure database (https://alphafold.ebi.ac.uk/), we performed protein-protein docking experiments. Since CDH26 is a transmembrane protein, we extracted the intracellular sequence of CDH26 (636-832) for the docking experiments (http://zdock.umassmed.edu/). We selected the top-scoring docking conformation and identified the binding sites using PDBePISA (https://www.ebi.ac.uk/msd-srv/prot_int/cgi-bin/piserver). The results indicated that amino acids 716-724, 787-794, and 802-817 of CDH26 are potential binding sites for STUB1 (Figure 6N). Therefore, we designed CDH26 mutants by deleting the segments 716-724, 787-794, and 802-817. Protein immunoprecipitation experiments revealed that deletion of these segments significantly weakened the binding of CDH26 to STUB1, while the binding of STUB1 to IL-4Rα was significantly enhanced (Figures 6O-6P). Our results suggest that the segments 716-724, 787-794, and 802-817 of CDH26 may be involved in its interaction

with STUB1 and competitively inhibit the binding of STUB1 to IL-4Rα. Together, our data suggest that CDH26 interacts with STUB1 to restrain the binding of STUB1 with IL-4Rα and its subsequent ubiquitination and degradation.

7. *Cdh26* siRNA encapsulated lipid nanoparticles effectively alleviates airway eosinophilia and mucus overproduction in the mouse model.

Finally, we sought to translate our findings into a therapeutic approach for asthma. We screened for efficient *Cdh26* siRNAs in 3T3 cells and encapsulated *Cdh26* siRNA-2 in lipid nanoparticles (LNPs) (Figure 7A). The encapsulation efficiency of *Cdh26* siRNA@LNPs was greater than 95%, with a zeta potential of -0.74mV (Table E2). We detected the cellular localization of DiR-labeled LNPs in BAL cells and lung tissue using immunofluorescence, and found that DiR-labeled LNPs were both uptaken by $Cd68^+$ macrophages and $Ccsp^+$ airway epithelial cells (Figures 7B-7C). To demonstrate the biodistribution of *Cdh26* siRNA@LNPs, we administered them intratracheally and used the In Vivo Imaging System (IVIS) to track the fluorescent signal of lipophilic carbocyanine $DiOC_{18}$ (DiR)-labeled LNPs. We found that LNPs could accumulate in the lung tissue for at least 3 days (Figure 7D).

We next intratracheally administered *Cdh26* siRNA@LNPs to mice sensitized and challenged with OVA (Figure 7E). H&E staining of liver, spleen, and kidney showed no significant damage following the administration of *Cdh26* siRNA@LNPs (Figure E10). Immunofluorescence staining of Cdh26 and Cd68 in BAL cells revealed a significant decrease of Cdh26 expression in $Cd68^+$ cells after *Cdh26* siRNA@LNPs treatment (Figure 7H). *Cdh26* siRNA@LNPs treatment significantly decreased the

number of eosinophils in BAL cells from OVA-challenged mice (Figure 7F). H&E and PAS staining revealed that *Cdh26* siRNA@LNPs treatment significantly decreased inflammation scores and the number of PAS staining-positive cells (Figures 7G-7I), suggesting that *Cdh26* siRNA@LNPs effectively inhibit airway eosinophilic inflammation and mucus overproduction in the mouse model. In addition, *Cdh26* siRNA@LNPs treatment significantly inhibited the transcript levels of *Arg1*, *Ym1*, *Ccl17*, and *Ccl24*, as well as the protein level of Arg1 (Figures 7J-7O). Our data suggest that *Cdh26* siRNA encapsulated lipid nanoparticles effectively alleviate airway eosinophilia and mucus overproduction in the mouse model.

Discussion:

IL-4R signaling drives mucous cell metaplasia, macrophage alternative activation, Th2 cell differentiation, and type 2 inflammation in allergic diseases (31-36). However, the mechanism underlying the regulation of IL-4R expression remains unclear. Our study uncovers a novel mechanism that CDH26 directly interacts with STUB1 and suppresses the STUB1-mediated ubiquitination-proteasomal degradation of IL-4Rα, a subunit shared by type I and type II IL-R, thus hampering the termination of IL-4R signaling and resulting in sustained activation of IL-4R signaling in asthma.

As a member of the cadherin family, CDH26 is highly expressed in allergic airway and gastrointestinal epithelium (24, 25). For the first time, we showed that CDH26 was upregulated in activated macrophages from eosinophilic asthma patients. Of note, CDH26 expression in sputum cells is higher in severe asthma compared to mild-moderate asthma as shown in Figure 1G, suggesting CDH26 may contribute to the

development of severe asthma. Several studies suggest a link between elevated number of M2 macrophages and asthma severity(37, 38). M2 macrophages can release chemokines such as CCL17 and CCL22 to recruit Th2 cells and amplify the Th2 cell response in asthma(39). Our in vivo and in vitro data demonstrated that macrophage-specific *Cdh26* deficiency suppresses airway eosinophilia, macrophage alternative activation and their secretion of CCL17 and CCL22, suggesting that CDH26-mediated macrophage alternative activation is essential in asthma pathogenesis.

CDH26 expression is upregulated in IL-13-stimulated epithelial cells(25). Here, we showed that IL-4 markedly increased CDH26 expression in mouse bone marrow-derived macrophages, while a selective JAK1 inhibitor suppressed CDH26 expression (Figures E11). This suggests that type 2 immune microenvironment may be responsible for CDH26 upregulation in macrophages. Interestingly, changes in DNA methylation can induce gene transcription and three hypomethylated sites were found in the CDH26 locus of asthma patients(40), suggesting epigenetic factor may also contribute to CDH26 upregulation in asthma patients.

The type 2 cytokines IL-4 and IL-13 activate IL-4R signaling in airway epithelial cells, macrophages, and lymphocytes, leading to mucous cell metaplasia, macrophages alternative activation, Th2 cell differentiation, and eosinophilic airway inflammation (12). We recently reported that CDH26 promotes mucus overproduction and the secretion of CCL11, CCL24, and CCL26 by airway epithelial cells via amplifying the type II IL-4R signaling (25). Airway epithelial cells mainly express type II IL-4R consisted of IL-4Rα and IL-13Rα1, while macrophages express type I IL4R composed

of IL-4Rα and IL-2Rγ (14). Here, we showed that CDH26 suppresses the degradation of IL-4Rα but not IL-2Rγ. Taken together, CDH26 upregulates the IL-4R signaling by inhibiting the protein degradation of IL-4Rα, a subunit shared by type I and type II IL-4R.

So far, the mechanisms underlying the regulation of IL-4R expression include endocytosis, ubiquitination-proteasome degradation, and co-receptor(16-18, 41) . Our results suggest that CDH26 regulates the degradation of IL-4Rα through ubiquitination-proteasome pathway, rather than endocytosis-lysosomal pathway. Ubiquitin-proteasome system is the main cellular protein degradation system(42). Ubiquitin molecules interact with protein substrates through the action of E1 ubiquitin-activating enzymes, E2 ubiquitin-conjugating enzymes, and E3 ubiquitin ligases. Wei and colleagues demonstrated the interaction between STUB1, an E3 ubiquitin ligase, and IL-4Rα promotes the ubiquitin-proteasomal degradation of IL-4Rα. *Stub1*-deficient mice exhibit spontaneous airway inflammation and macrophages alternative activation (17). In the present study, we demonstrated that CDH26 directly interacts with STUB1 and suppresses the binding of STUB1 to IL-4Rα, thereby restrains STUB1-mediated IL-4Rα ubiquitination and proteasomal degradation. This novel mechanism can explain our observation that *Cdh26* deficiency suppressed IL-4-induced macrophages alternative activation and our recent reports that *CDH26* knockdown inhibited IL-13-induced mucus production and chemokine expression by epithelial cells.

Besides IL-4Rα, STUB1 is involved in the ubiquitination-proteasomal degradation of multiple protein molecules including EGFR and PKM2(43, 44). We

observed that CDH26 can inhibit the degradation of EGFR (unpublished data), and EGFR pathway plays an important role in airway remodeling in asthma (45). Taken our findings together, the highly expressed CDH26 in airway epithelium and macrophages of asthma patients is a promising therapeutic target. In addition, the observation that CDH26 expression is even higher in severe asthma compared to mild-moderate asthma suggests targeting CDH26 may be beneficial for patients with severe asthma.

Lipid nanoparticles have been widely utilized for the delivery of mRNA vaccines (46). Recent studies on lipid nanoparticles have shown that modified lipid nanoparticles can effectively penetrate the mucus-cilia barrier maintaining high stability in nebulized form (47). Our LNPs encapsulating *Cdh26* siRNA effectively suppressed OVA-induced eosinophilic airway inflammation and macrophage alternative activation in mice. LNPs encapsulating *CDH26* siRNA may represent a new method for treating eosinophilic asthma.

Our study has several limitations. First, our asthma patients are mild-moderate asthma, CDH26 expression and localization in severe asthma needs to be further investigated. Second, we cannot exclude the possibility that CDH26 may interact with other E3 ubiquitin ligase besides STUB1 as shown in Figure 6C to prevent IL-4Rα degradation. Third, although we identified the putative binding domain between CDH26 and STUB1, the specific binding site needs to be identified. Finally, the efficacy and safety of LNPs encapsulating *Cdh26* siRNA and its aerosolized form in asthma requires further study.

In summary, we demonstrated that CDH26 directly interacts with STUB1 and

restrains the binding of STUB1 to IL-4Rα, thereby suppressing IL-4Rα ubiquitination-proteasomal degradation, leading to sustained activation of IL-4R signaling, alternative activation of macrophage, and airway inflammation in asthma. Lipid nanoparticles encapsulating *Cdh26* siRNA can effectively alleviate macrophage activation and airway eosinophilia in mice.

Table 1 Subject characteristics

	Controls	Non-eosinophilic asthma	Eosinophilic asthma	P value (Control vs. asthma)	P value (Eos vs. non-Eos)
Number	17	7	25		
Age, y	41.41±9.179	46.71±12.46	41.08±11.75	0.9709	0.3064
Sex, M: F, %F	11:6,64.7	3:4,42.9	11:14,44	0.3333	0.3333
Body mass index	21.95±2.587	24.4±5.244	23.94±3.776	0.0551	0.929
FEV_1% predicted	93.8±10.18	88.17±14.94	77.7±21.03	0.0105	0.447
FVC% predicted	96.98±14.24	104.3±16.73	99.17±11.57	0.3815	0.8586
Sputum eosinophil, %	2.735±9.039	0.6186±1.145	20.12±15.06	< 0.0001	< 0.0001
BALF eosinophil, %	0.8063±2.263	14.83±24.11	14.67±14.5	< 0.0001	0.3967

Serum IgE, IU/mL	44.25±47.25	32.48±23.38	191.6±144.9	0.0327	0.0326
FeNO, ppb	22.47±12.84	29.86±26.11	94.26±58.91	0.0043	0.0032
Blood eosinophil, #	0.07±0.0587 4	0.2014±0.42 76	0.4276±0.37 7	< 0.0001	0.0587
Blood eosinophil, %	1.259±1.135	3.829±4.441	6.628±5.076	< 0.0001	0.1117

Note: Values were presented as mean ± SD.

Abbreviations: FEV1, forced expiratory volume in the first second; FEV1, forced vital capacity; BALF, bronchoalveolar lavage fluid; FeNO, fraction of exhaled nitric oxide.

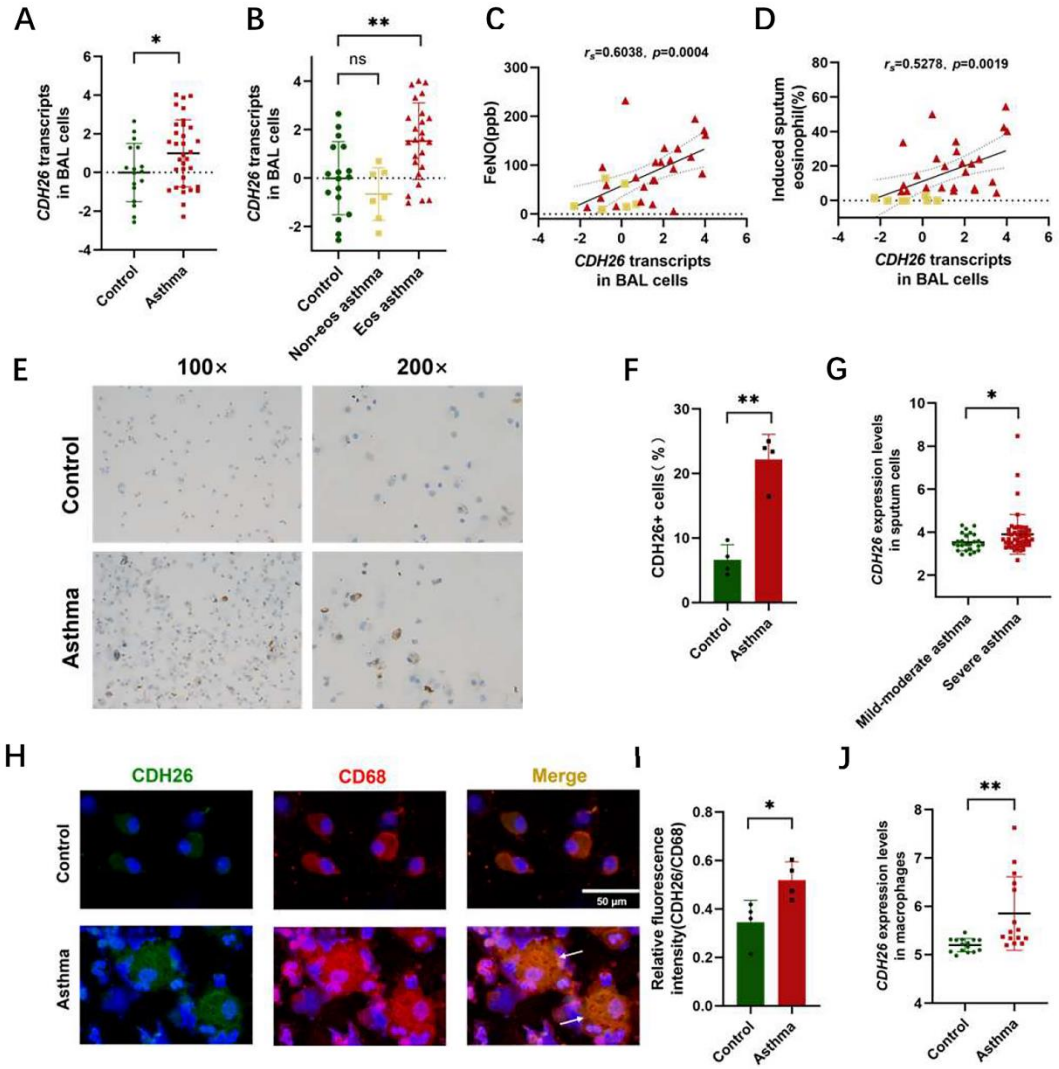

1. CDH26 expression is upregulated in lung macrophages from eosinophilic asthma patients.

A-B) *CDH26* transcript levels in BAL cells from eosinophilic asthmatics (n=25), non-eosinophilic asthmatics (n=7) and control subjects (n=17) were measured by quantitative PCR. The transcript levels were expressed as log2 transformed and relative to the mean value for control subjects. C-D) Spearman's correlation assays between

CDH26 transcripts in BAL cells and FeNO, induced sputum eosinophil (%) of asthma patients. E) Representative images of CDH26 immumohistochemical staining in BAL cells from asthmatics (n=4) and control subjects (n=4). F) The proportion of $CDH26^{+}$ cells in BAL cells from asthma patients (n=4) and control subjects (n=4). G) The expression levels of *CDH26* in a microarray data (GSE76262) using sputum cells from subjects with mild-moderate (n=25) and severe asthma (n=49) were analyzed. H-I) Representative images for immunofluorescence staining of CDH26 (green) and CD68 (red) in BAL cells from asthma patients (n=4) and control subjects (n=4). Arrows indicate enlarged, foamy, and granular macrophages. Nuclei was stained with DAPI (blue). Quantification for relative immunofluorescent intensity of CDH26 compared to CD68 was performed using ImageJ. J) The expression of CDH26 in isolated alveolar macrophages from asthma patients and control subjects (GSE2125). E-F) Data are mean ± SD. *p<0.05; **p<0.01. Abbreviations: CDH26, cadherin-26; FeNO, fraction of exhaled nitric oxide.

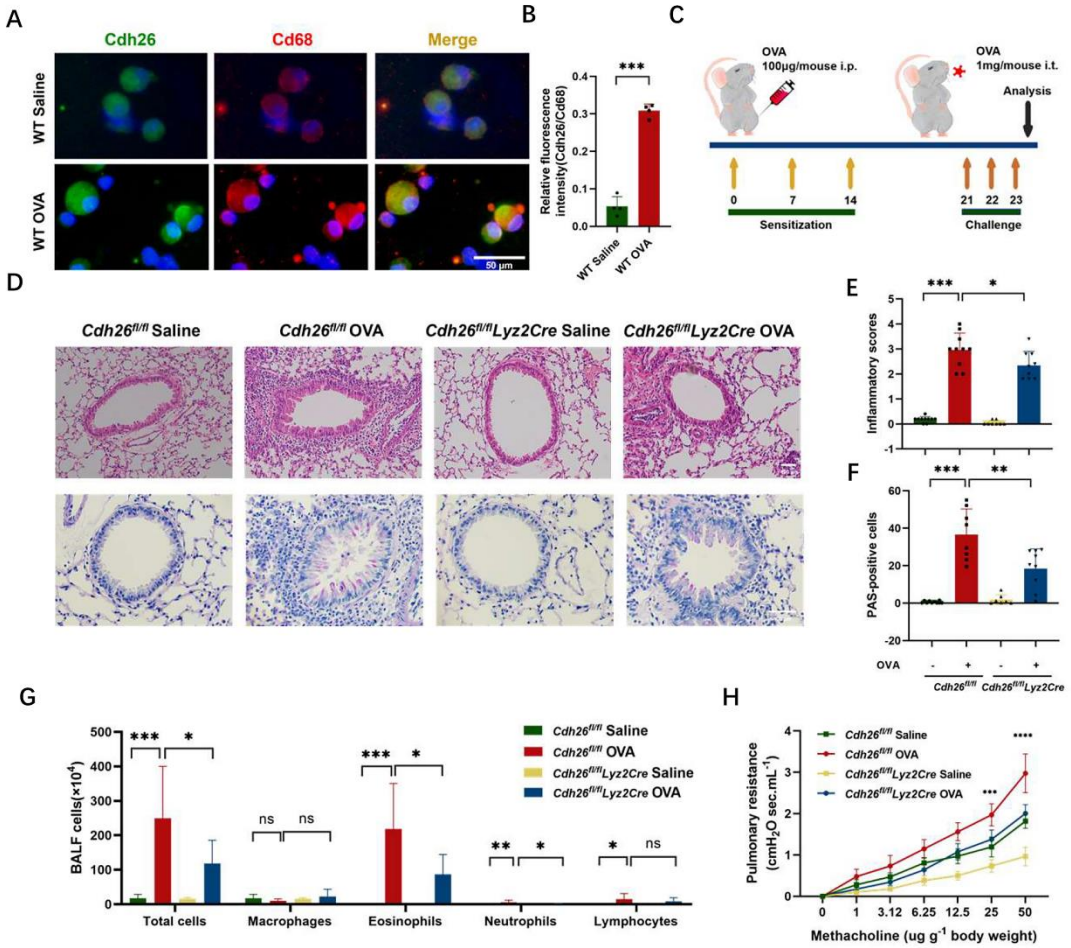

2. Macrophage-specific *Cdh26* deficiency alleviates airway eosinophilia and mucus overproduction in a mouse model of allergic airway inflammation.

A-B) Representative images for co-immunofluorescence staining of Cdh26 (green) and Cd68 (red) in BAL cells from mouse (scale bar = 50 μm). Quantification of relative immunofluorescence intensity of Cdh26 to Cd68 (n=4). C) Mouse experimental schedule. D) Representative images of H&E and PAS staining in mouse lung sections (scale bar = 100 μm). E) The inflammatory score was graded in four random fields for each lung section at 200× magnification. F) The numbers of PAS-staining-positive cells were counted in four random fields for each lung section at 200× magnification. G) Cell counts for macrophages, eosinophils, lymphocytes and neutrophils in BALF. H)

Pulmonary resistance in response to different concentrations of intravenous methacholine in mice. n=8-10 mice per group. Data are mean ± SD. *p<0.05; **p<0.01; ***p<0.001. Abbreviations: Cdh26, cadherin-26; Cd68, Cd68 molecule; WT, wild type; OVA, ovalbumin; H&E staining, hematoxylin-eosin staining; PAS staining, periodic acid-Schiff; BAL, bronchoalveolar lavage.

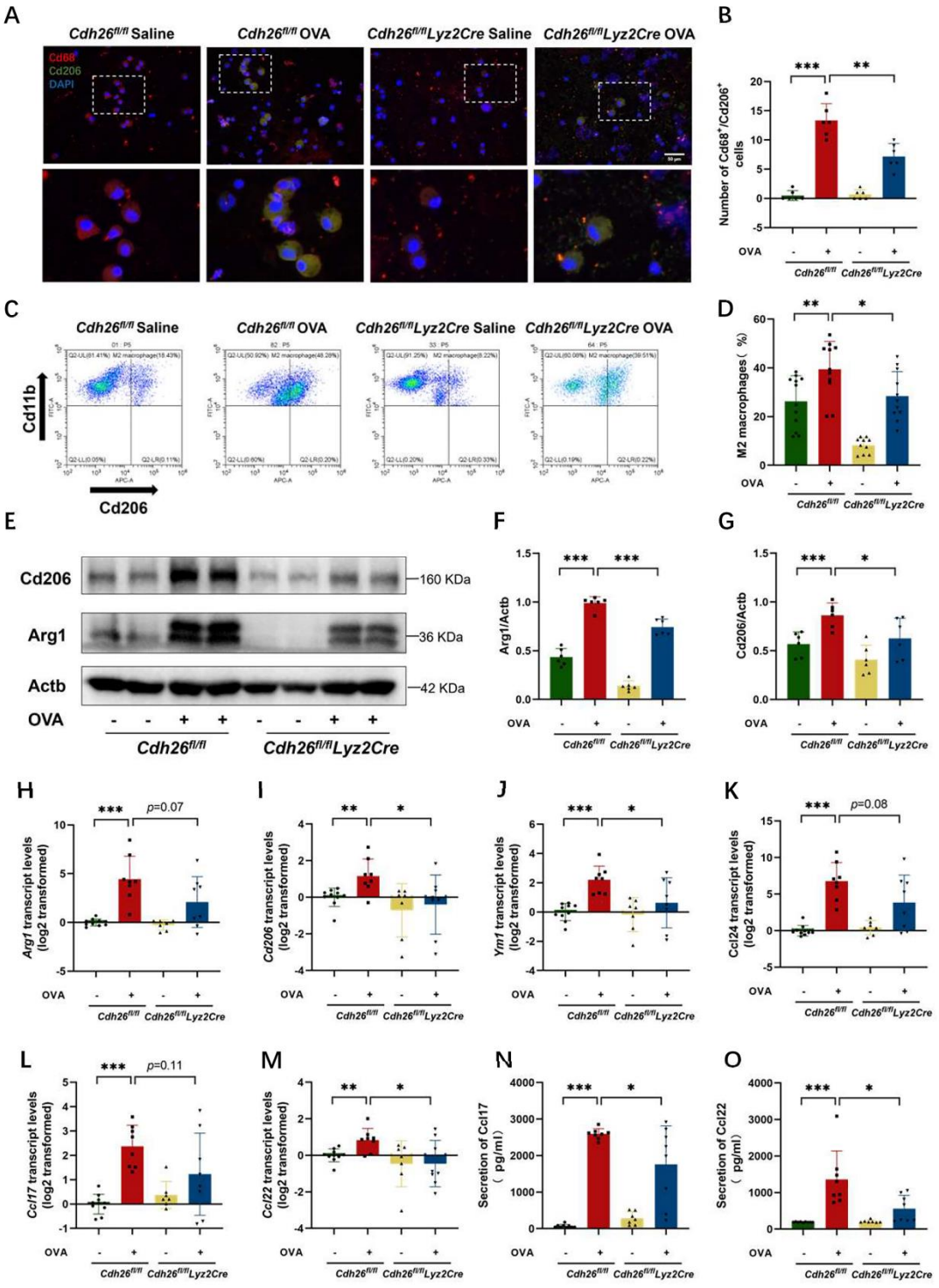

3. Cdh26 is required for macrophage alternative activation.

A) Representative images for immunofluorescence staining of Cd206 (green) and Cd68 (red) in BAL cells from mouse (scale bar = 50 μm). Nuclei was stained with DAPI

(blue). B) The numbers of $Cd68^+/Cd206^+$ cells were counted in the cytospin of BAL cells in 5 fields for each mouse and the average number were calculated (n = 6 mice) using ImageJ. C) Flow cytometry for M2 macrophages using single cell suspensions from mouse lung tissue. $Cd45^+Cd11b^+$ cells were identified as macrophages, and $Cd45^+Cd11b^+Cd206^+$ cells were identified as M2 macrophages. Representative dot plots showing the percentages of M2 macrophages in different groups. D) The percentages of M2 macrophages of total macrophages in different groups. E-G) The protein levels of Arg1, Cd206 in mouse lungs (n=6) were determined by western blotting and representative image was shown. Densitometry assay was performed using ImageJ, and Arg1, Cd206 protein levels were indexed to Actb. H-M) The mRNA levels of *Cd206*, *Ym1*, *Arg1*, *Ccl24*, *Ccl17* and *Ccl22* in mouse lungs were determined using quantitative PCR. The transcript levels were expressed as log2 transformed and relative to the mean value of control group. N-Q) The protein levels of Ccl17, Ccl22 in the supernatant of BAL fluid were determined using ELISA. n=8-10 mice per group. Data are mean ± SD. *p<0.05; **p<0.01; ***p<0.001. Abbreviations: Cd68, Cd68 molecule; Cd206, mannose receptor C-type 1; Arg1, arginase-1; Ym1, also named as Chil3, chitinase-like protein 3; Ccl17, C-C motif chemokine ligand 17; Ccl22, C-C motif chemokine ligand 22; Ccl24, C-C motif chemokine ligand 24; Actb, actin beta.

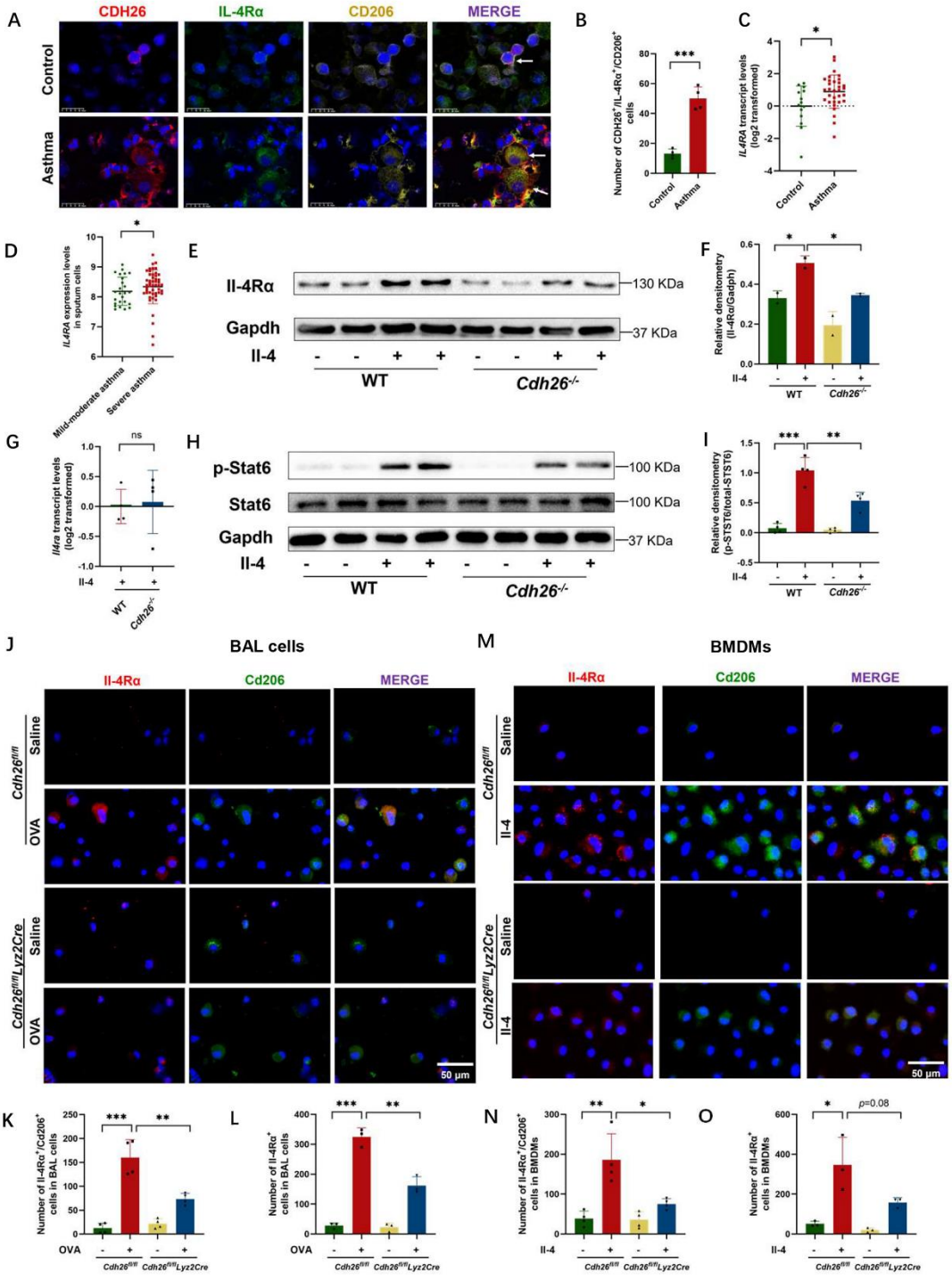

4. *Cdh26* deficiency suppresses IL-4R expression and IL-4R-STAT6 signaling in macrophages.

A) Representative images of immunostaining of CDH26 (red), IL-4Rα (green) and CD206 (yellow) in BAL cells from asthma patients (n=4) and control subjects (n=4).

Nuclei was stained with DAPI (blue). B) The numbers of CDH26^{+}/IL-4Rα $^{+}$/CD206^{+} cells were counted in the cytospin of BAL cells in 5 fields for each subject and the average number were calculated using ImageJ (n = 4 per group). C) *IL4RA* transcript levels in induced sputum cells from asthma patients (n=32) and control subjects (n=14) were determined by quantitative PCR. The transcript levels were expressed as log2 transformed and relative to the mean value for control subjects. D) The expression levels of *IL4RA* in a microarray data (GSE76262) using sputum cells from subjects with mild-moderate (n=25) and severe asthma (n=49) were analyzed. E-F) The protein levels of Il-4Rα in BMDM cells exposed to Il-4 for 48h were determined by western blotting. Densitometry assay was performed using ImageJ, and Il-4Rα protein levels were indexed to Gapdh. G) The transcript levels of *Il4ra* in Il-4 stimulated BMDMs derived from WT or *Cdh26*$^{-/-}$ mice were determined by quantitative PCR. The transcript levels were expressed as log2 transformed and relative to the mean value for control group. H-I) The protein levels of p-STAT6 in WT or *Cdh26*$^{-/-}$ mice derived-BMDM cells stimulated with or without Il-4 for 6h were determined by western blotting. Densitometry assay was performed using ImageJ, and p-STAT6 protein levels were indexed to total STAT6. J) Representative images for immunofluorescence staining of Il-4Rα (green) and Cd206 (red) in BAL cells from *Cdh26*$^{fl/fl}$*Lyz2Cre* and *Cdh26*$^{fl/fl}$ mice challenged with saline or OVA. Nuclei was stained with DAPI (blue). K-L) The numbers of Il-4Rα^{+}Cd206^{+} cells (K), Il-4Rα^{+} (L) were counted in the cytospin of BAL cells in 5 fields for each mouse and the average number were calculated for *Cdh26*$^{fl/fl}$*Lyz2Cre* and *Cdh26*$^{fl/fl}$ mice challenged with saline or OVA using ImageJ (n =

4 mice per group). M) Representative images for immunofluorescence staining of Il-4Rα (green) and Cd206 (red) in saline- or Il-4-stimulated BMDMs derived from *Cdh26*$^{fl/fl}$*Lyz2Cre* and *Cdh26*$^{fl/fl}$ mice. Nuclei was stained with DAPI (blue). N-O) The numbers of Il-4Rα^{+}Cd206^{+}(N), Il-4Rα^{+}(O) cells were counted in saline- or Il-4-stimulated BMDMs derived from *Cdh26*$^{fl/fl}$*Lyz2Cre* and *Cdh26*$^{fl/fl}$ mice using ImageJ (n=4 wells per group). Data are mean ± SD. **p*<0.05; ***p*<0.01; ****p*<0.001. Abbreviations: CDH26, cadherin-26; CD206, mannose receptor C-Type 1; IL-4Rα, interleukin-4 receptor subunit alpha; BAL, bronchoalveolar lavage; BMDM, bone marrow derived macrophage; STAT6, signal transducer and activator of transcription 6; Gapdh, glyceraldehyde-3-phosphate dehydrogenase.

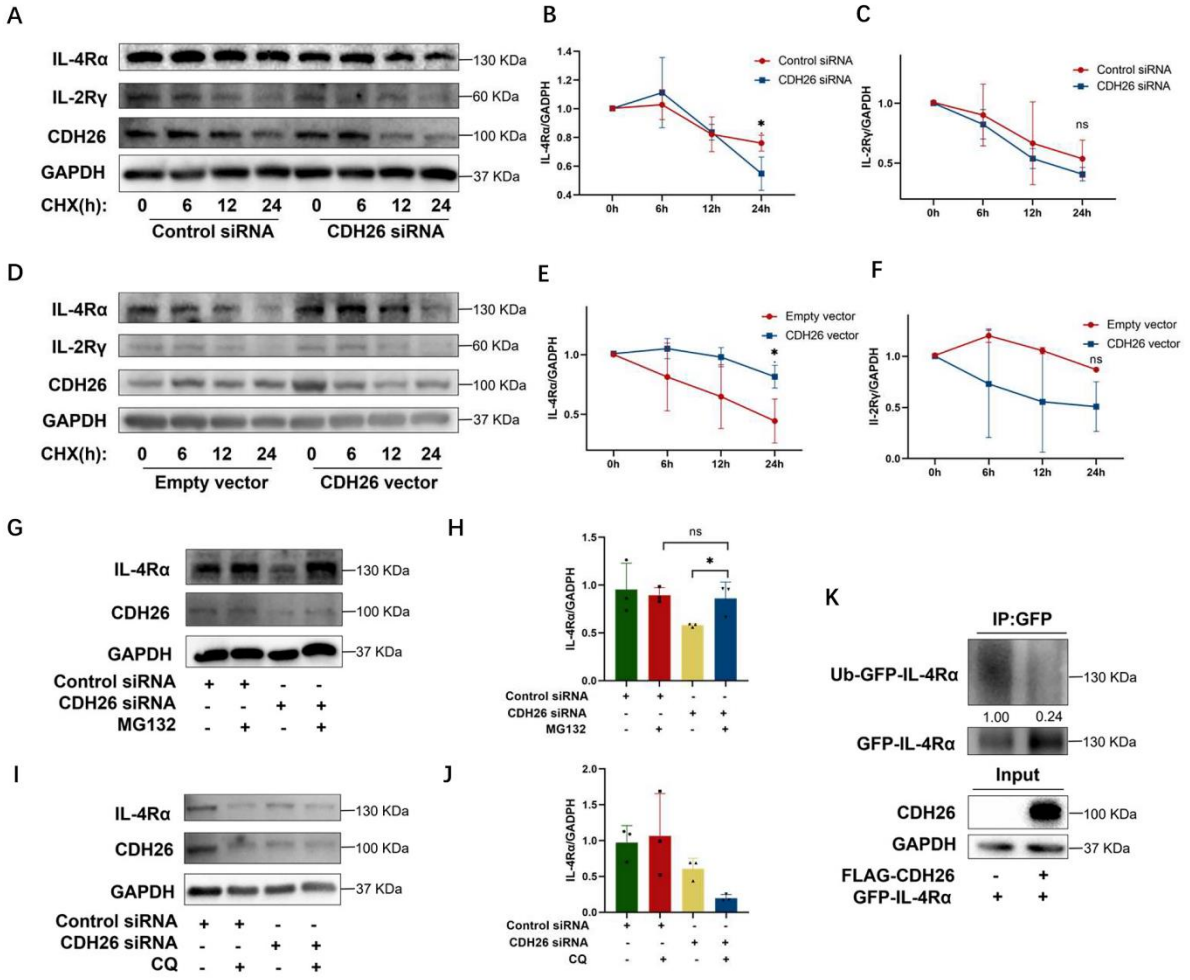

5. CDH26 enhances IL-4Rα expression via inhibiting its ubiquitination and degradation.

A-C) IL-4Rα and IL-2Rγ protein levels were measured in A549 cells transfected with control or CDH26 siRNA and treated with CHX for 0, 6, 12, 24h using western blotting. Densitometry assay was performed using ImageJ, and IL-4Rα and IL-2Rγ protein levels were indexed to GAPDH. D-F) IL-4Rα and IL-2Rγ protein levels were measured in A549 cells transfected with empty or CDH26 overexpressing vector and treated with CHX for 0, 6, 12, 24h using western blotting. Densitometry assay was performed using ImageJ, and IL-4Rα and IL-2Rγ protein levels were indexed to GAPDH. The experiment was repeated 3 times independently. G-H) IL-4Rα protein level was determined in A549 cells transfected with control or CDH26 siRNA and

treated with MG132 using western blotting. Densitometry assay was performed using ImageJ, and IL-4Rα protein levels were indexed to GAPDH. I-J) IL-4Rα protein level was determined in A549 cells transfected with control or CDH26 siRNA and treated with CQ using western blotting. Densitometry assay was performed using ImageJ, and IL-4Rα protein level was indexed to GAPDH. K) HEK-293T cells were transfected with plasmids expressing IL-4Rα^{GFP} and CDH26^{FLAG} as indicated, and cell lysates were immunoprecipitated with anti-GFP antibody followed by western blotting. The ubiquitination level of IL-4Rα was assessed using ubiquitin antibodies. All experiments were repeated for at least three times independently. Data are mean ± SD. *p<0.05. Abbreviations: CDH26, cadherin-26; IL-4Rα, interleukin-4 receptor subunit alpha; IL-2Rγ, interleukin-2 receptor subunit gamma; GAPDH, glyceraldehyde-3-phosphate dehydrogenase; CHX, cycloheximide; MG132, Z-Leu-Leu-Leu-al; CQ, chloroquine.

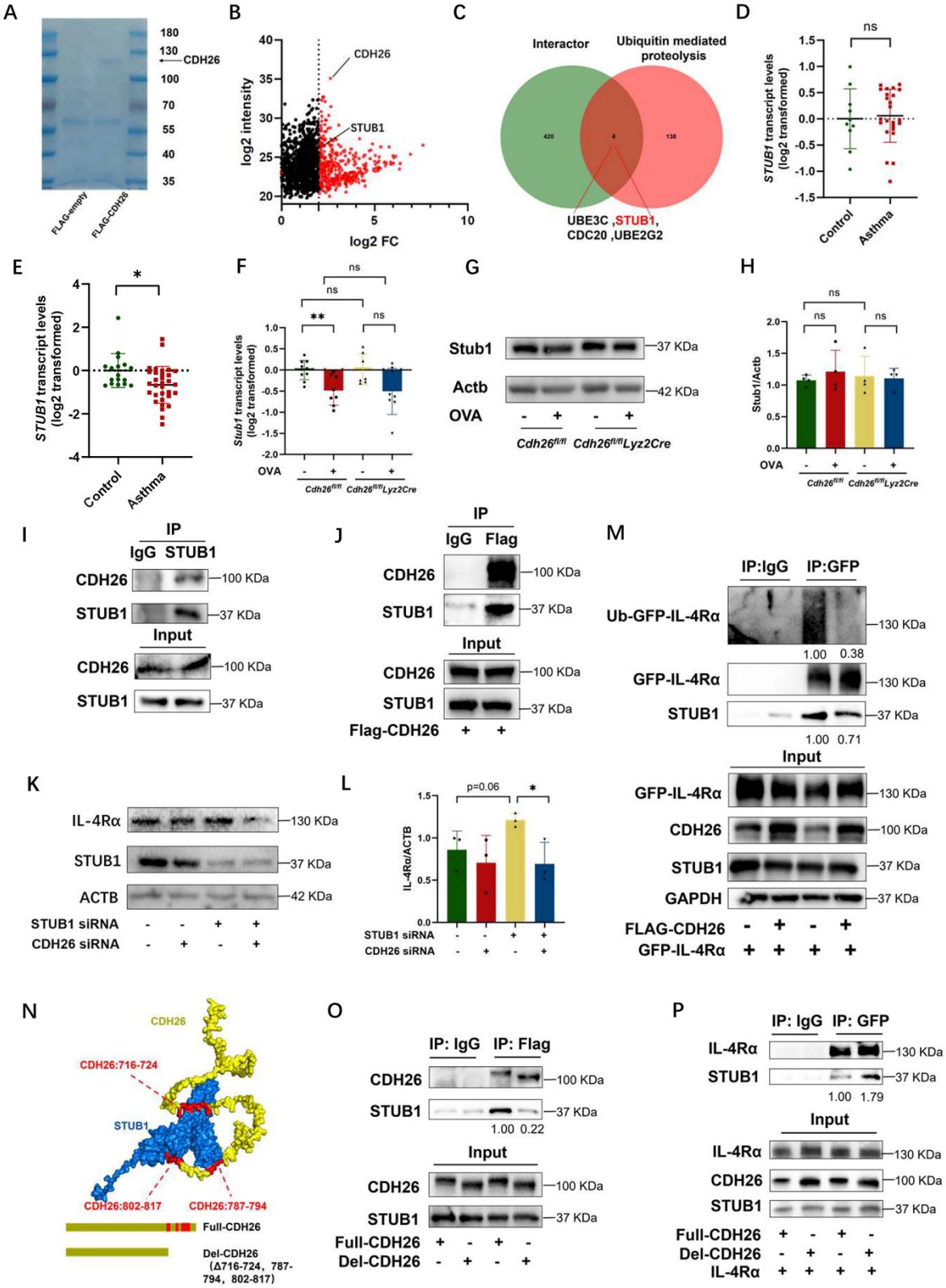

6. CDH26 interacts with STUB1 to restrain the binding of STUB1 with IL-4Rα.

A) HEK-293T cells were transfected with plasmids expressing $CDH26^{FLAG}$, and cell lysates were immunoprecipitated with anti-FLAG antibody followed by mass spectrum. B) Volcanic map of the proteins interacting with CDH26 detected by mass spectrum. C) Veen diagram shown the protein molecules identified by intersecting the proteins interacting with CDH26 and the proteins involved in ubiquitin-mediated proteolysis. D) *STUB1* transcript levels in bronchial brushings from asthma patients (n=24) and control subjects (n=10) were determined using quantitative PCR. E) *STUB1* transcript levels in BAL cells from asthma patients (n=32) and control subjects (n=17) were determined using quantitative PCR. F) The transcript levels of *Stub1* in lungs of $Cdh26^{fl/fl}Lyz2Cre$ or $Cdh26^{fl/fl}$ mice challenged with saline or OVA were determined using quantitative PCR (n = 8-10 mice per group). The transcript levels were expressed as log2 transformed and relative to the mean value of control group. G-H) The protein levels of Stub1 in lungs of $Cdh26^{fl/fl}Lyz2Cre$ or $Cdh26^{fl/fl}$ mice challenged with saline or OVA were determined using western blotting (n = 3 per group). Densitometry assay was performed using ImageJ, and Stub1 protein levels were indexed to Actb. I) Binding of CDH26 with STUB1 was examined using immunoprecipitation assay. J) Binding of IL-4Rα with STUB1 was examined using immunoprecipitation assay. K-L) A549 cells were treated with CDH26 siRNA and/or STUB1 siRNA, and IL-4Rα protein levels were determined using western blotting. Densitometry assay was performed using ImageJ, and IL-4Rα protein level was indexed to GAPDH. The experiment was repeated 3 times independently. M) HEK-293T cells were transfected with plasmids expressing $IL\text{-}4R\alpha^{GFP}$ and $CDH26^{FLAG}$ as indicated, and cell lysates were immunoprecipitated with anti-GFP or IgG antibody followed by western blotting. The ubiquitination level of IL-4Rα was assessed using ubiquitin antibodies. N) The binding

interface between CDH26 (716-724, 787-794, and 802-817) and STUB1 was predicted based on the molecular docking model using zdock. O) HEK-293T cells were transfected with plasmids expressing full-CDH26 (1-832) and del-CDH26^{FLAG} (deleting amino acids 716-724, 787-794, and 802-817), and cell lysates were immunoprecipitated with anti-FLAG or IgG antibody followed by western blotting. P) HEK-293T cells were transfected with plasmids expressing IL-4Rα^{GFP}, full-CDH26 and del-CDH26^{FLAG}, and cell lysates were immunoprecipitated with anti-GFP or IgG antibody followed by western blotting. Data are mean ± SD. *p<0.05. Abbreviations: CDH26, cadherin-26; STUB1, STIP1 homology and U-box containing protein 1; ACTB, actin beta; GAPDH, glyceraldehyde-3-phosphate dehydrogenase; IL-4Rα, interleukin-4 receptor subunit alpha.

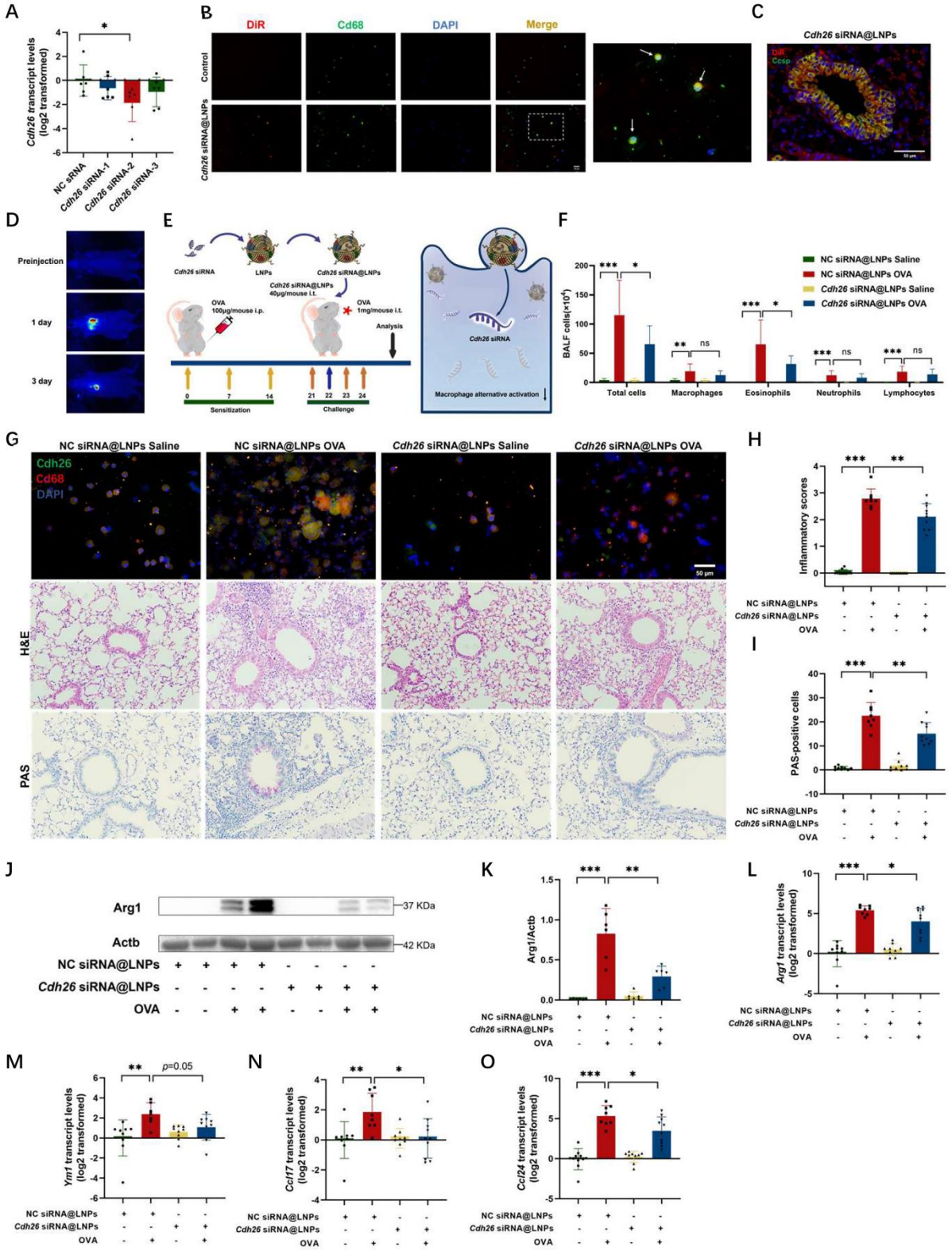

7. *Cdh26* siRNA encapsulated lipid nanoparticles effectively alleviates airway eosinophilia and mucus overproduction in the mouse model.

A) *Cdh26* transcripts in 3T3 cells transfected with three Cdh26 siRNA were measured by quantitative PCR. The transcript levels were expressed as log2 transformed and relative to the mean value for control group. B) Representative images for immunofluorescence staining of DiR (red) and Cd68 (green) in mouse BAL cells. C) Representative images for immunofluorescence staining of DiR (red) and Ccsp (green) in mouse lung sections. D) Representative IVIS images of the mouse administrated with DiR-labeled *Cdh26* siRNA@LNPs. E) Mouse experimental schedule. F) Cell counts for macrophages, eosinophils, lymphocytes and neutrophils in BALF. G) Representative images of immunofluorescence staining of Cdh26 (green) and Cd68 (green) in BAL cells, H&E staining, and PAS staining in mouse lung sections. H) The inflammatory score was graded in four random fields for each lung section at 200× magnification. I) The numbers of PAS-staining-positive cells were counted in four random fields for each lung section at 200× magnification. J-K) The protein levels of Arg1 in mouse lungs were determined by western blotting, and Arg protein levels were indexed to Actb. L-O) The transctipt levels of *Cd206*, *Arg1*, *Ym1*, *Ccl17* and *Ccl24* in mouse lungs were determined using quantitative PCR. The transcript levels were expressed as log2 transformed and relative to the mean value for control group. n=8-10 mice per group. Data are mean ± SD. *p<0.05; **p<0.01; ***p<0.001. Abbreviations: CDH26, cadherin-26; BALF, bronchoalveolar lavage fluid; LNPs, lipid nanoparticles; DiR, $DiOC_{18}$; Cd68, Cd68 molecule; Ccsp, club cells 10 kDa secretory protein; Arg1, arginase-1; Ym1, also named as Chil3, chitinase-like protein 3; Ccl24, C-C motif chemokine ligand 24; Ccl17, C-C motif chemokine ligand 17.

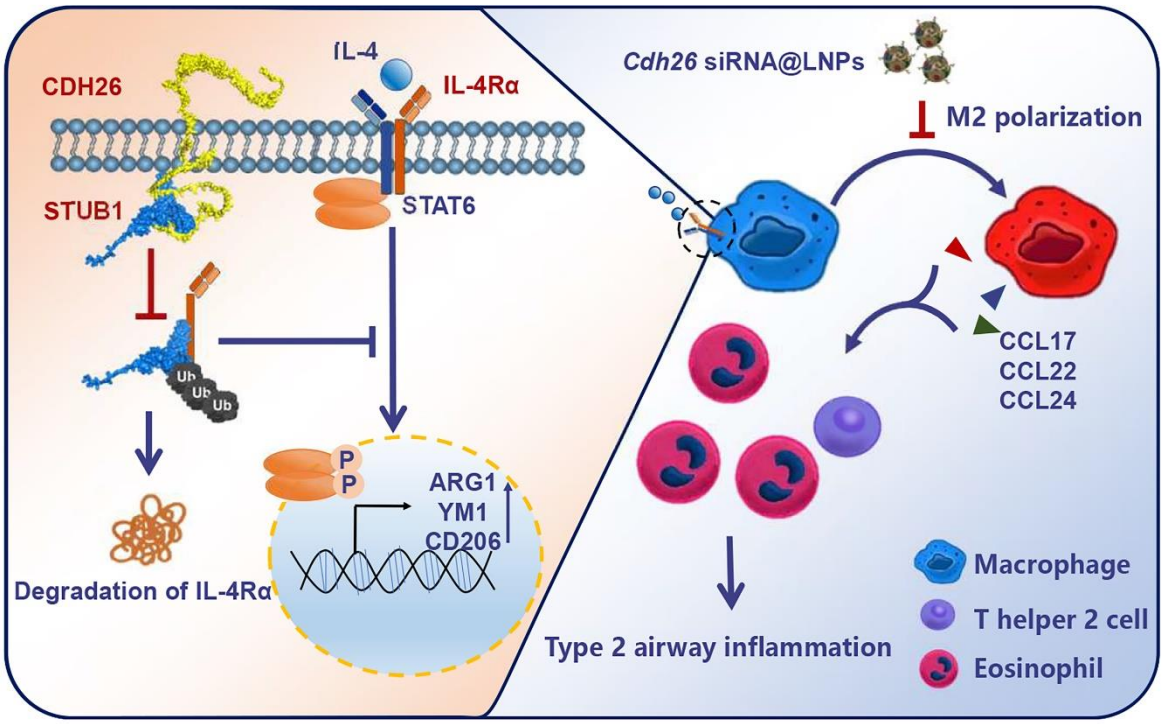

8. Diagrams of CDH26 promotes macrophage alternative activation via suppressing STUB1-mediated IL-4Rα ubiquitination in asthma.

CDH26, through interacting with STUB1 and trapping it, inhibits IL-4Rα ubiquitination-proteasomal degradation, leading to sustained activation of the IL-4R-STAT6 signaling, macrophage alternative activation, and type 2 inflammation in asthma. Lipid nanoparticles encapsulating *Cdh26* siRNA can effectively alleviate OVA-induced macrophage M2 polarization and airway inflammation in mice.

Reference

1. Lambrecht BN, Hammad H. The immunology of asthma. *Nature immunology* 2015; 16: 45-56.

2. Tan LD, Alismail A, Ariue B. Asthma guidelines: comparison of the National Heart, Lung,

and Blood Institute Expert Panel Report 4 with Global Initiative for Asthma 2021. *Current opinion in pulmonary medicine* 2022; 28: 234-244.

3. Schoettler N, Strek ME. Recent Advances in Severe Asthma: From Phenotypes to Personalized Medicine. *Chest* 2020; 157: 516-528.

4. Shaw DE, Sousa AR, Fowler SJ, Fleming LJ, Roberts G, Corfield J, Pandis I, Bansal AT, Bel EH, Auffray C, Compton CH, Bisgaard H, Bucchioni E, Caruso M, Chanez P, Dahlén B, Dahlen SE, Dyson K, Frey U, Geiser T, Gerhardsson de Verdier M, Gibeon D, Guo YK, Hashimoto S, Hedlin G, Jeyasingham E, Hekking PP, Higenbottam T, Horváth I, Knox AJ, Krug N, Erpenbeck VJ, Larsson LX, Lazarinis N, Matthews JG, Middelveld R, Montuschi P, Musial J, Myles D, Pahus L, Sandström T, Seibold W, Singer F, Strandberg K, Vestbo J, Vissing N, von Garnier C, Adcock IM, Wagers S, Rowe A, Howarth P, Wagener AH, Djukanovic R, Sterk PJ, Chung KF. Clinical and inflammatory characteristics of the European U-BIOPRED adult severe asthma cohort. *The European respiratory journal* 2015; 46: 1308-1321.

5. Aegerter H, Lambrecht BN, Jakubzick CV. Biology of lung macrophages in health and disease. *Immunity* 2022; 55: 1564-1580.

6. Yunna C, Mengru H, Lei W, Weidong C. Macrophage M1/M2 polarization. *European journal of pharmacology* 2020; 877: 173090.

7. Shapouri-Moghaddam A, Mohammadian S, Vazini H, Taghadosi M, Esmaeili SA, Mardani F, Seifi B, Mohammadi A, Afshari JT, Sahebkar A. Macrophage plasticity, polarization, and function in health and disease. *Journal of cellular physiology* 2018; 233: 6425-6440.

8. Becerra-Díaz M, Strickland AB, Keselman A, Heller NM. Androgen and Androgen Receptor as Enhancers of M2 Macrophage Polarization in Allergic Lung Inflammation. *Journal of immunology (Baltimore, Md : 1950)* 2018; 201: 2923-2933.

9. Zhong Y, Huang T, Huang J, Quan J, Su G, Xiong Z, Lv Y, Li S, Lai X, Xiang Y, Wang Q, Luo L, Gao X, Shao Y, Tang J, Lai T. The HDAC10 instructs macrophage M2 program via deacetylation of STAT3 and promotes allergic airway inflammation. *Theranostics* 2023; 13: 3568-3581.

10. Saradna A, Do DC, Kumar S, Fu QL, Gao P. Macrophage polarization and allergic asthma. *Translational research : the journal of laboratory and clinical medicine* 2018; 191: 1-14.

11. Zhang P, Miska J, Heimberger AB. GLUT3 regulates alternative macrophage signaling through a glucose transport-independent role. *The Journal of clinical investigation* 2023; 133.

12. Chatila TA. Interleukin-4 receptor signaling pathways in asthma pathogenesis. *Trends in molecular medicine* 2004; 10: 493-499.

13. Park SJ, Lee KP, Kang S, Lee J, Sato K, Chung HY, Okajima F, Im DS. Sphingosine 1-phosphate induced anti-atherogenic and atheroprotective M2 macrophage polarization through IL-4. *Cellular signalling* 2014; 26: 2249-2258.

14. Junttila IS, Mizukami K, Dickensheets H, Meier-Schellersheim M, Yamane H, Donnelly RP, Paul WE. Tuning sensitivity to IL-4 and IL-13: differential expression of IL-4Ralpha, IL-13Ralpha1, and gammac regulates relative cytokine sensitivity. *The Journal of experimental medicine* 2008; 205: 2595-2608.

15. Harb H, Chatila TA. Mechanisms of Dupilumab. *Clinical and experimental allergy : journal of the British Society for Allergy and Clinical Immunology* 2020; 50: 5-14.

16. Bai JY, Li Y, Xue GH, Li KR, Zheng YF, Zhang ZQ, Jiang Q, Liu YY, Zhou XZ, Cao C. Requirement of Gαi1 and Gαi3 in interleukin-4-induced signaling, macrophage M2 polarization and allergic asthma response. *Theranostics* 2021; 11: 4894-4909.

17. Wei Q, Sha Y, Bhattacharya A, Abdel Fattah E, Bonilla D, Jyothula SS, Pandit L, Khurana Hershey GK, Eissa NT. Regulation of IL-4 receptor signaling by STUB1 in lung inflammation. *American journal of respiratory and critical care medicine* 2014; 189: 16-29.

18. Moshkovits I, Karo-Atar D, Itan M, Reichman H, Rozenberg P, Morgenstern-Ben-Baruch N, Shik D, Ejarque-Ortiz A, Hershko AY, Tian L, Coligan JE, Sayós J, Munitz A. CD300f associates with IL-4 receptor α and amplifies IL-4-induced immune cell responses. *Proceedings of the National Academy of Sciences of the United States of America* 2015; 112: 8708-8713.

19. Koning H, Sayers I, Stewart CE, de Jong D, Ten Hacken NH, Postma DS, van Oosterhout AJ, Nawijn MC, Koppelman GH. Characterization of protocadherin-1 expression in primary bronchial epithelial cells: association with epithelial cell differentiation. *FASEB journal : official publication of the Federation of American Societies for Experimental Biology* 2012; 26: 439-448.

20. Lachowicz-Scroggins ME, Gordon ED, Wesolowska-Andersen A, Jackson ND, MacLeod HJ, Sharp LZ, Sun M, Seibold MA, Fahy JV. Cadherin-26 (CDH26) regulates airway epithelial cell cytoskeletal structure and polarity. *Cell discovery* 2018; 4: 7.

21. Woodruff PG, Boushey HA, Dolganov GM, Barker CS, Yang YH, Donnelly S, Ellwanger A, Sidhu SS, Dao-Pick TP, Pantoja C, Erle DJ, Yamamoto KR, Fahy JV. Genome-wide profiling identifies epithelial cell genes associated with asthma and with treatment response to corticosteroids. *Proceedings of the National Academy of Sciences of the United States of America* 2007; 104: 15858-15863.

22. Blanchard C, Mingler MK, Vicario M, Abonia JP, Wu YY, Lu TX, Collins MH, Putnam PE, Wells SI, Rothenberg ME. IL-13 involvement in eosinophilic esophagitis: transcriptome analysis and reversibility with glucocorticoids. *The Journal of allergy and clinical immunology* 2007; 120: 1292-1300.

23. Li RW, Gasbarre LC. A temporal shift in regulatory networks and pathways in the bovine small intestine during Cooperia oncophora infection. *International journal for parasitology* 2009; 39: 813-824.

24. Caldwell JM, Collins MH, Kemme KA, Sherrill JD, Wen T, Rochman M, Stucke EM, Amin L, Tai H, Putnam PE, Jiménez-Dalmaroni MJ, Wormald MR, Porollo A, Abonia JP, Rothenberg ME. Cadherin 26 is an alpha integrin-binding epithelial receptor regulated during allergic inflammation. *Mucosal immunology* 2017; 10: 1190-1201.

25. Feng Y, Chen S, Xiong L, Chang C, Wu W, Chen D, Gao J, Chen G, Yi L, Zhen G. Cadherin-26 Amplifies Airway Epithelial IL-4 Receptor Signaling in Asthma. *American journal of respiratory cell and molecular biology* 2022; 67: 539-549.

26. Barcellos VA, Dos Santos VCH, Moreira MÂ F, Dalcin PTR. Asthma control and sputum eosinophils in adult patients: a cross-sectional study in southern Brazil. *Scientific reports* 2023; 13: 21464.

27. Siracusa MC, Reece JJ, Urban JF, Jr., Scott AL. Dynamics of lung macrophage activation in response to helminth infection. *Journal of leukocyte biology* 2008; 84: 1422-1433.

28. Kuo CS, Pavlidis S, Loza M, Baribaud F, Rowe A, Pandis I, Sousa A, Corfield J, Djukanovic R, Lutter R, Sterk PJ, Auffray C, Guo Y, Adcock IM, Chung KF. T-helper cell type 2 (Th2) and non-Th2 molecular phenotypes of asthma using sputum transcriptomics in U-BIOPRED. *The European respiratory journal* 2017; 49.

29. Woodruff PG, Koth LL, Yang YH, Rodriguez MW, Favoreto S, Dolganov GM, Paquet AC, Erle DJ. A distinctive alveolar macrophage activation state induced by cigarette smoking. *American journal of respiratory and critical care medicine* 2005; 172: 1383-1392.

30. Liao W, Foo HYC, Tran TNQ, Chai CLL, Wong WSF. Calcaratarin D, a labdane diterpenoid, attenuates mouse asthma via modulating alveolar macrophage function. *British journal of pharmacology* 2023; 180: 1056-1071.

31. Wang X, Hallen NR, Lee M, Samuchiwal S, Ye Q, Buchheit KM, Maxfield AZ, Roditi RE, Bergmark RW, Bhattacharyya N, Ryan T, Gakpo D, Raychaudhuri S, Dwyer D, Laidlaw TM, Boyce JA, Gutierrez-Arcelus M, Barrett NA. Type 2 inflammation drives an airway basal stem cell program through insulin receptor substrate signaling. *The Journal of allergy and clinical immunology* 2023; 151: 1536-1549.

32. Nagasaki T, Schuyler AJ, Zhao J, Samovich SN, Yamada K, Deng Y, Ginebaugh SP, Christenson SA, Woodruff PG, Fahy JV, Trudeau JB, Stoyanovsky D, Ray A, Tyurina YY, Kagan VE, Wenzel SE. 15LO1 dictates glutathione redox changes in asthmatic airway epithelium to worsen type 2 inflammation. *The Journal of clinical*

investigation 2022; 132.

33. Boomer J, Choi J, Alsup A, McGregor MC, Lieu J, Johnson C, Hall C, Shi X, Kim T, Goss C, Lew D, Christenson S, Woodruff PG, Hastie A, Mauger D, Wenzel SE, Hoffman EA, Schechtman KB, Castro M. Increased Muc5AC and Decreased Ciliated Cells in Severe Asthma Partially Restored by Inhibition of IL-4Rα Receptor. *American journal of respiratory and critical care medicine* 2024.
34. Wang BF, Cao PP, Norton JE, Poposki JA, Klingler AI, Suh LA, Carter R, Huang JH, Bai J, Stevens WW, Tan BK, Peters AT, Grammer LC, Conley DB, Welch KC, Liu Z, Kern RC, Kato A, Schleimer RP. Evidence that oncostatin M synergizes with IL-4 signaling to induce TSLP expression in chronic rhinosinusitis with nasal polyps. *The Journal of allergy and clinical immunology* 2023; 151: 1379-1390.e1311.
35. Avlas S, Shani G, Rhone N, Itan M, Dolitzky A, Hazut I, Grisaru-Tal S, Gordon Y, Shoda T, Ballaban A, Ben-Baruch NM, Rochman M, Diesendruck Y, Nahary L, Bitton A, Halpern Z, Benhar I, Varol C, Rothenberg ME, Munitz A. Epithelial cell-expressed type II IL-4 receptor mediates eosinophilic esophagitis. *Allergy* 2023; 78: 464-476.
36. Kuperman DA, Huang X, Koth LL, Chang GH, Dolganov GM, Zhu Z, Elias JA, Sheppard D, Erle DJ. Direct effects of interleukin-13 on epithelial cells cause airway hyperreactivity and mucus overproduction in asthma. *Nature medicine* 2002; 8: 885-889.
37. Han X, Huang S, Xue P, Fu J, Liu L, Zhang C, Yang L, Xia L, Sun L, Huang SK, Zhou Y. LncRNA PTPRE-AS1 modulates M2 macrophage activation and inflammatory diseases by epigenetic promotion of PTPRE. *Science advances* 2019; 5: eaax9230.

38. Xia L, Wang X, Liu L, Fu J, Xiao W, Liang Q, Han X, Huang S, Sun L, Gao Y, Zhang C, Yang L, Wang L, Qian L, Zhou Y. lnc-BAZ2B promotes M2 macrophage activation and inflammation in children with asthma through stabilizing BAZ2B pre-mRNA. *The Journal of allergy and clinical immunology* 2021; 147: 921-932.e929.

39. Staples KJ, Hinks TS, Ward JA, Gunn V, Smith C, Djukanović R. Phenotypic characterization of lung macrophages in asthmatic patients: overexpression of CCL17. *The Journal of allergy and clinical immunology* 2012; 130: 1404-1412.e1407.

40. Forno E, Wang T, Qi C, Yan Q, Xu CJ, Boutaoui N, Han YY, Weeks DE, Jiang Y, Rosser F, Vonk JM, Brouwer S, Acosta-Perez E, Colón-Semidey A, Alvarez M, Canino G, Koppelman GH, Chen W, Celedón JC. DNA methylation in nasal epithelium, atopy, and atopic asthma in children: a genome-wide study. *The Lancet Respiratory medicine* 2019; 7: 336-346.

41. Amano Y, Yamashita Y, Kojima K, Yoshino K, Tanaka N, Sugamura K, Takeshita T. Hrs recognizes a hydrophobic amino acid cluster in cytokine receptors during ubiquitin-independent endosomal sorting. *The Journal of biological chemistry* 2011; 286: 15458-15472.

42. Çetin G, Klafack S, Studencka-Turski M, Krüger E, Ebstein F. The Ubiquitin-Proteasome System in Immune Cells. *Biomolecules* 2021; 11.

43. Peng W, Shi S, Zhong J, Liang H, Hou J, Hu X, Wang F, Zhang J, Geng S, Sun X, Zhong D, Cui H. CBX3 accelerates the malignant progression of glioblastoma multiforme by stabilizing EGFR expression. *Oncogene* 2022; 41: 3051-3063.

44. Zhao G, Yuan H, Li Q, Zhang J, Guo Y, Feng T, Gu R, Ou D, Li S, Li K, Lin P. DDX39B

drives colorectal cancer progression by promoting the stability and nuclear translocation of PKM2. *Signal transduction and targeted therapy* 2022; 7: 275.

45. Habibovic A, Hristova M, Heppner DE, Danyal K, Ather JL, Janssen-Heininger YM, Irvin CG, Poynter ME, Lundblad LK, Dixon AE, Geiszt M, van der Vliet A. DUOX1 mediates persistent epithelial EGFR activation, mucous cell metaplasia, and airway remodeling during allergic asthma. *JCI insight* 2016; 1: e88811.

46. Zong Y, Lin Y, Wei T, Cheng Q. Lipid Nanoparticle (LNP) Enables mRNA Delivery for Cancer Therapy. *Advanced materials (Deerfield Beach, Fla)* 2023; 35: e2303261.

47. Jiang AY, Witten J, Raji IO, Eweje F, MacIsaac C, Meng S, Oladimeji FA, Hu Y, Manan RS, Langer R, Anderson DG. Combinatorial development of nebulized mRNA delivery formulations for the lungs. *Nature nanotechnology* 2024; 19: 364-375.

Cadherin-26 drives macrophage alternative activation via suppressing STUB1-mediated IL-4Rα ubiquitination in asthma

Gongqi Chen[1,2,3], Shengchong Chen[1,2,3], Chunli Huang[1,2,3], Wei Gu[1,2,3], Huiru Jie[1,2,3], Lu Zhao[1,2,3], Weiqiang Kong[1,2,3], Jiali Gao[1,2,3], Yuchen Feng[1,2,3], Lingling Yi[1,2,3], Guohua Zhen[1, 2,3]

[1]Division of Respiratory and Critical Care Medicine, Department of Internal Medicine, Tongji Hospital, Tongji Medical College, Huazhong University of Science and Technology, Wuhan 430030, China; [2]Key Laboratory of Respiratory Diseases, National Health Commission of the People's Republic of China; [3] National Clinical Research Center for Respiratory Diseases, Wuhan, China

Correspondence to: Guohua Zhen, Division of Respiratory and Critical Care Medicine, Tongji Hospital, Wuhan, China 430030; Email: ghzhen@tjh.tjmu.edu.cn

Supplementary Materials and Methods, Figures and Tables

Extensive Materials and Methods Section.

Supplementary Figures:

Supplementary Tables:

Table E1. Primers for quantitative PCR.

Table E2 The characterization of LNPs.

Extensive Materials and Methods Section:

Subjects

We recruited 17 control subjects, 25 eosinophilic asthma patients (sputum eosinophils > 3%), and 7 non-eosinophilic asthma patients (sputum eosinophil ≤ 3%) (1). All participants were Chinese and recruited from Tongji Hospital. None of the participants had a history of smoking or received inhaled or oral corticosteroids or leukotriene antagonists. For each participant, we collected demographic information and induced sputum samples. We also measured spirometry, fractional exhaled nitric oxide (FeNO), and serum IgE levels. All asthma patients had a history of episodic wheezing and met the criteria for bronchial hyperresponsiveness, with a methacholine PD20 of less than 2.505 mg or a 12% or greater increase in forced expiratory volume in the first second (FEV1) after the inhalation of 200 μg of salbutamol. All participants also underwent bronchoalveolar lavage fluid (BALF) collection. The control subjects had no history of chest tightness or wheezing, and lung function stimulation tests were negative. All participants provided written informed consent, and the study was approved by the ethics committee of Tongji Hospital, Huazhong University of Science and Technology.

Murine model of allergic airway inflammation

Cdh26$^{fl/fl}$*Lyz2Cre* mice on a C57BL/6N background were constructed from the GemPharmatech (Nanjing, China). Exon 4 of *Cdh26* gene was knocked out in *Cdh26*$^{fl/fl}$*Lyz2Cre* mice. All experimental mice were sensitized three times on days 0, 7, and 14 by intraperitoneal injection of sensitizing agents (OVA + aluminum hydroxide mixture) at a volume of 200 μl

(containing 100 μg OVA). From days 21 to 23, each mouse was intranasally stimulated with 50 μl of OVA solution (containing 1 mg OVA) daily (2). Pulmonary resistance in response to various intravenous methacholine concentrations was measured using the forced oscillation technique with the FlexiVent system (SCIREQ) 24 hours after the final challenge. Bronchoalveolar lavage fluid (BALF) was collected and cell counts for macrophages, eosinophils, lymphocytes, and neutrophils were determined as previously described (3). Lung tissues were collected for histological analysis, quantitative PCR, western blotting, flow cytometry, and immunostaining. All experimental procedures were approved by the Animal Care and Use Committee of Tongji Hospital, Huazhong University of Science and Technology.

Cell culture and treatment

BMDM (bone marrow-derived macrophages) cells and mouse pulmonary macrophages were isolated from both WT (wild-type) and *Cdh26*$^{-/-}$ mice. They were then treated with IL-4 for 48 hours. HEK-293T and A549 cells were cultured in DMEM medium supplemented with 10% FBS (Biological Industries, Israel). These cells were transfected with either scrambled control or CDH26 siRNA (80 nM; GeneCopoeia) or empty or CDH26 cDNA expression vector (500 ng/mL) using Lipofectamine 3000 (Invitrogen, CA).

Quantitative PCR

Total RNA was isolated from induced sputum cells, BAL cells, mouse lungs, mouse pulmonary macrophages and BMDM cells using TRIzol (Takara, Tokyo, Japan). The isolated RNA was then reverse transcribed into cDNA using the PrimeScript RT reagent kit (Takara, Tokyo, Japan). The primer sequences for gene amplification were obtained from the primer bank and can be found in Table S1. The expression levels of these genes were determined using

the 2−ΔΔCT method. The gene expression values were expressed as log2 transformed and relative to the median expression level of the control group.

Western blotting

The protein sample preparation involved several steps. Firstly, the cells were lysed using ice-cold RIPA lysis buffer (Servicebio, Wuhan, China) supplemented with EDTA-free Protease Inhibitor Cocktail Tablets. The lysates were then subjected to SDS-PAGE, either 8% or non-reducing, for protein separation. The proteins were subsequently transferred onto a PVDF membrane (Roche, Mannheim, Germany) by electrophoresis. Next, the PVDF membranes were blocked using a solution containing Tris-buffered saline with Tween-20 and nonfat milk. The membranes were then incubated overnight at 4 °C with specific antibodies at a dilution of 1:1000 in 5% milk. Antibodies used in western blotting were: anti-CDH26 mAb (Sigma-Aldrich, 1:1000 dilution), mouse anti-Il-4Rα mAb (R&D system, 1:1000 dilution), human anti-IL-4Rα mAb (Abcam, 1:1000 dilution), anti-IL-2Rγ mAb (Abclonal, 1:1000 dilution), anti-total and phosphorylated Stat6 pAb (Cell Signaling, 1:1,000 dilution), anti-STUB1 mAb (Abcam, 1:1000 dilution), mouse anti-Cd206 mAb (R&D system, 1:1000 dilution) and anti-ARG1 mAb (Proteintech, 1:1000 dilution), anti-FLAG mAb (Proteintech, 1:2000 dilution) , anti-GFP mAb (Proteintech, 1:2000 dilution), anti-ubiquitin pAb (Proteintech, 1:1000 dilution), anti- anti-GAPDH pAb (Proteintech, 1:4000 dilution) and anti- anti-ACTB pAb (Proteintech, 1:4000 dilution). After the overnight incubation, the membranes were treated with a horseradish peroxidase-conjugated goat anti-rabbit secondary antibody for 1 hour at room temperature. Finally, the protein signals were detected using an ECL kit according to the manufacturer's instructions.

Histology staining

The left lungs of mice were fixed by inflation and embedded in paraffin. 5-μm sections were then cut from the embedded tissues. These sections were subjected to H&E staining, PAS staining, and Masson staining. For H&E staining, lung sections were treated with hematoxylin and eosin staining kit (Servicebio, Wuhan, China) to evaluate peri-bronchial inflammation. The severity of inflammation surrounding airways with a luminal diameter of 170 ± 40 μm in H&E-stained lung sections was assessed using the following scoring system: 0 for normal; 1 for few cells; 2 for a single layer of inflammatory cells; 3 for 2-4 layers of inflammatory cells; and 4 for more than 4 layers of inflammatory cells. For PAS staining, lung sections were stained using a periodic acid-Schiff staining kit (Servicebio, Wuhan, China) to detect mucus. The number of PAS-positive cells in airways with a luminal diameter of 170 ± 40 μm was counted in five randomly selected fields per lung section at 200× magnification.

Immunofluorescence

The immunofluorescence method of frozen slides was as follows: After the slides were restored to room temperature, they were washed 3 times with PBS for 5 min each time. The immunostaining permeabilization buffer was added and incubated at room temperature for 20 min. Add goat serum blocking buffer and block for 30 minutes. Subsequently, the slices were incubated with primary antibodies in a wet box overnight at 4°C. Antibodies used in immunofluorescence were: anti-CDH26 mAb (Sigma-Aldrich, 1:100 dilution), mouse anti-Il-4Rα mAb (R&D system, 1:200 dilution), human anti-IL-4Rα mAb (R&D 1:200 dilution), anti-CD206 mAb (Proteintech, 1:2000 dilution) and anti-CD68 mAb (Proteintech, 1:2000 dilution). Antibody wash buffer was added to remove the primary antibody, and then the Cy3 or FITC

conjugated secondary antibodies (donkey-anti mouse or rabbit IgG, Abbkine) were added and incubated at room temperature for 1 h. After PBS cleaning, DAPI staining is used. Washing again, the slices were sealed with anti-fluorescence quenching sealing agent. Then, slices were observed under fluorescence microscope within one week to avoid fluorescence quenching, and images were collected.

Flow cytometry

Following euthanasia, the lung samples of mice were dissected in HBSS buffer. Single-cell suspensions were prepared by filtering the samples through a 100 μm nylon filter strainer and washing them in HBSS buffer supplemented with 2% FBS, 20 mM HEPES, and 5 mM EDTA. The cells were then resuspended at a concentration of 1*10^6 cells/100 μL. Subsequently, 100 μL of the cell suspension was added to a flow tube, and 2 μL of FcBlock was added to each tube, followed by incubation on ice for 10 min. Three types of tubes were set up: a blank tube, a single staining tube, and a sample tube. In the single staining tube, a single antibody was added. In the sample tube, 0.5 μL of LIVE/DEAD™ Fixable Yellow Dead Cell Stain Kit (Invitrogen, USA), 2 μL of anti-Cd45 (bv510), and 1.25 μL of anti-Cd11b (FITC) antibodies (Biolegend, USA) were added, followed by incubation on ice for 15-20 min while protected from light. After permeabilization with intracellular Staining Permeabilization Wash Buffer Biolegend, USA), 1.5 μL of anti-Cd206 (PE) antibody was added and incubated for 20 min. Finally, the cells were suspended in PBS and analyzed promptly.

ELISA

Ccl17 and Ccl22, in BALF were analyzed by ELISA (BOSTER Biological Technology, China). ELISA was performed according to the manufacturer's instructions. All samples and

standards were measured in duplicate.

Immunoprecipitation

NHK 293T cell proteins were extracted using RIPA lysis buffer (Sigma-Aldrich). An appropriate dilution of either anti-FLAG mAb (Proteintech, 1:550 dilution) or anti-GFP mAb (Proteintech, 1:50 dilution) was added to a centrifuge tube coated with Protein G. The antibody-bead mixture was incubated at 4°C for 4 hours using a tube rotator. Then, 50 μg of cell lysates were added to the mixture, and the lysate-bead/antibody conjugate mixtures were incubated overnight at 4°C. The mixtures were subsequently resuspended in 5×SDS loading buffer, boiled for 5 minutes, and analyzed by Western blotting.

Mass spectrometry analysis

We transfected HEK-293T cells with CDH26-FLAG overexpression plasmid. The samples were obtained through co-immunoprecipitation experiments using the FLAG antibody. Beads samples were incubated in the reaction buffer (1% SDC/100 mM Tris-HCl, pH 8.5/10 mM TCEP/40 mM CAA) at 95 °C for 10 min for protein denaturation, cysteine reduction and alkylation. The eluates were diluted with equal volume of H_2O and subjected to trypsin digestion overnight by adding trypsin at a ratio of 1:50 (enzyme: protein, w/w) for overnight digestion at 37 °C. The next day, TFA was used to bring the pH down to 6.0 to end the digestion. After centrifugation (12000×g, 15 min), The peptide was purified using self-made SDB desalting columns. The eluate was vacuum dried and stored at -20 °C for later use. Mass spectrometry (MS) data acquisition was carried out on a Q Exactive HF mass spectrometer coupled with UltiMate 3000 RSLCnano system. Peptides were loaded through auto-sampler and separated in a C18 analytical column (75μm × 25cm, C18, 1.9μm, 100Å). Mobile phase A

(0.1% formic acid) and mobile phase B (80% ACN, 0.1% formic acid) were used to establish the separation gradient. A constant flow rate was set at 300 nL/min. For DDA mode analysis, each scan cycle is consisted of one full-scan mass spectrum (R = 60 K, AGC = 3e6, max IT = 20 ms, scan range = 350–1800 m/z) followed by 20 MS/MS events (R = 15 K, AGC = 2e5, max IT = 50 ms). HCD collision energy was set to 28. Isolation window for precursor selection was set to 1.6 Da. Former target ion exclusion was set for 30 s. MS raw data were analyzed with MaxQuant (V1.6.6) using the Andromeda database search algorithm. Spectra files were searched against Human database (2022-03-29,20377 entries) using the following parameters: LFQ mode was checked for quantification; Variable modifications, Oxidation (M), Acetyl (Protein N-term) & Deamidation (NQ); Fixed modifications, Carbamidomethyl (C); Digestion, Trypsin/P; The MS1 match tolerance was set as 20 ppm for the first search and 4.5 ppm for the main search; the MS2 tolerance was set as 20 ppm. Search results were filtered with 1% FDR at both protein and peptide levels. Proteins denoted as decoy hits, contaminants, or only identified by sites were removed, the remaining identifications were used for further quantification analysis. Proteins with a fold change > 4 between bait IP and control were screened out as interactors of the bait protein.

Preparation of *Cdh26* siRNA encapsulated lipid nanoparticles

Cdh26 siRNA encapsulated lipid nanoparticles were prepared by Cynbio (Shanghai, China). The preparation method is as follows: *Cdh26* siRNA was dissolved in RNase-Free water. For the aqueous phase, a siRNA working solution was prepared using 100 mM sodium acetate (pH 4.0), with a concentration of 0.35 mg/mL. For the organic phase, a lipid mixture was prepared in anhydrous ethanol at a concentration of 25 mM, with the following composition:

DLin-MC3-DMA: DSPC: Cholesterol: DMPE-PEG2000 = 50:10:38.5:1.5. The encapsulation of *Cdh26* siRNA into lipids was performed using the PNI Ignite instrument with the Ignite microfluidic chip, at a total flow rate of 12 mL/min and a water-to-organic ratio of 3:1. After encapsulation, the nanoparticles were diluted with 10 times the volume of DPBS (calcium and magnesium free). The diluted mixture was then centrifuged at 4°C and 3000 g for 30 minutes using a 100 kDa ultrafiltration tube, until the volume before dilution was reached. The buffer was replaced with DPBS three times, achieving a displacement rate of 99%. A sucrose solution of the corresponding concentration was prepared using DPBS, and the *Cdh26* siRNA encapsulated lipid nanoparticles were diluted with a 5% sucrose solution. The encapsulation efficiency, particle size, PDI, and zeta potential were measured. Finally, the *Cdh26* siRNA encapsulated lipid nanoparticles were stored at -80°C.

Statistical analysis

Data analysis was conducted using Prism version 8 (GraphPad Software). For normally distributed data, we calculated the means ± standard deviation (SD) and performed parametric tests such as Student's t-test or one-way ANOVA followed by Tukey's multiple comparison test for group comparisons. For non-normally distributed data, we calculated medians with interquartile ranges and utilized non-parametric tests, such as the Mann-Whitney test. Spearman correlation coefficient was used to assess correlation. Statistical significance was defined as $p < 0.05$.

Supplementary Figures:

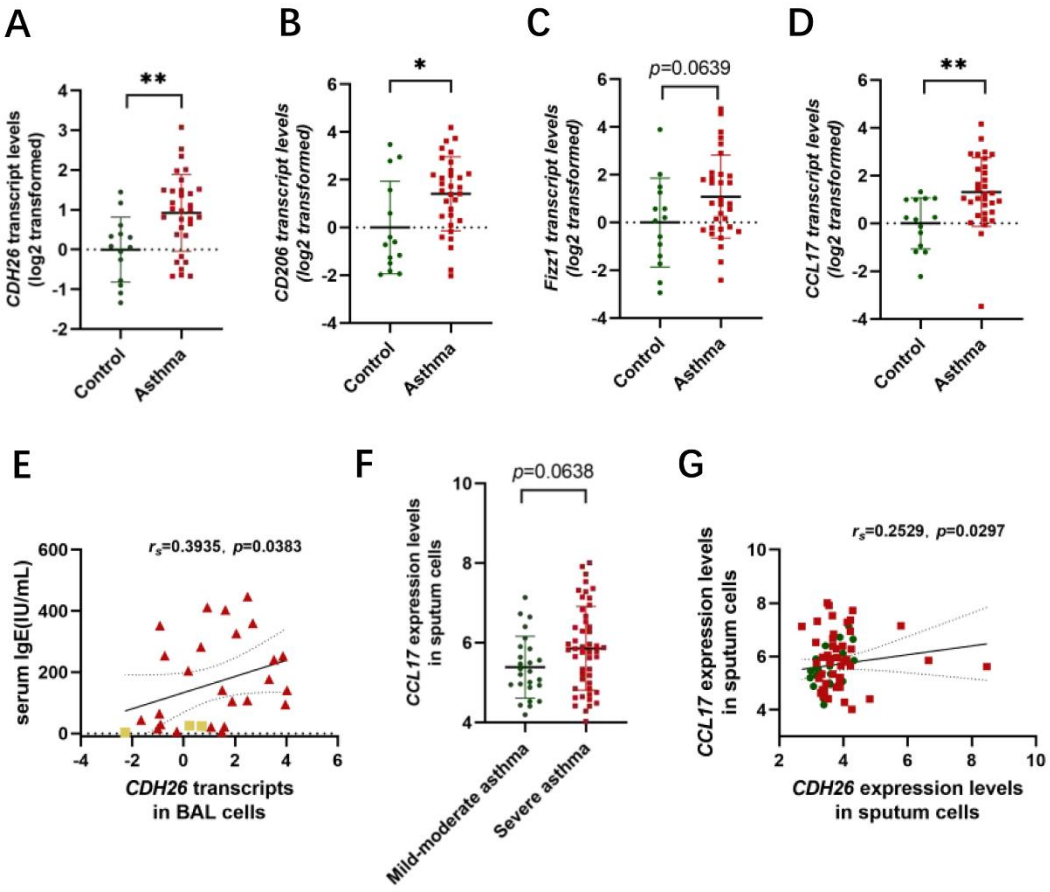

Figure E1 *CDH26*, *CD206*, *FIZZ1* and *CCL17* transcript levels in induced sputum cells of asthma patients.

A-D) *CDH26*, *CD206*, *FIZZ1* and *CCL17* transcript levels in induced sputum cells from asthma patients (n=32) and control subjects (n=14) were measured by quantitative PCR. The transcript levels were expressed as log2 transformed and relative to the mean value for control group. E) Spearman's correlation assays between *CDH26* transcripts in BAL cells and serum IgE of asthma patients. F) The expression of CCL17 in induced sputum array data (GSE76262). G) Spearman's correlation assays between *CDH26* and *CCL17* expression levels in asthma patients in induced sputum array data. Data are mean ± SD. *p<0.05; **p<0.01. Abbreviations: CDH26,

cadherin-26; CD206, mannose receptor C-Type 1; Fizz1, found in inflammatory zone 1; CCL17, C-C motif chemokine ligand 17.

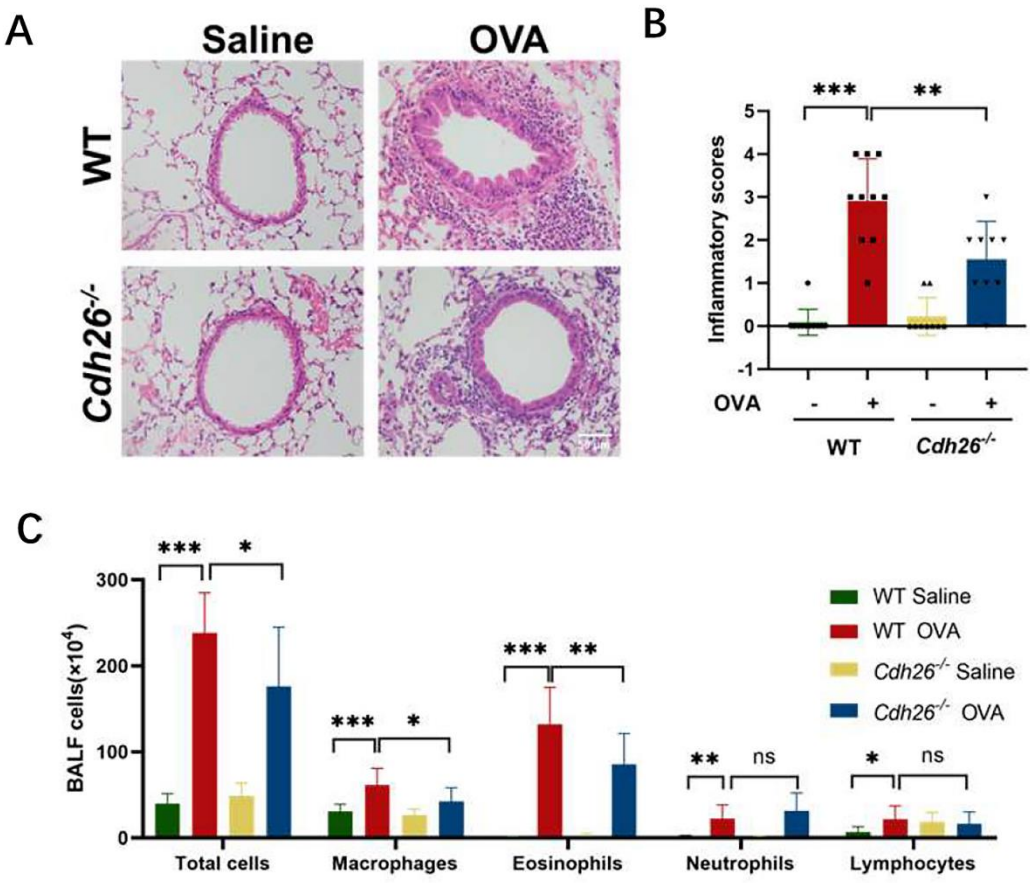

Figure E2 *Cdh26* deficiency abrogated lung inflammation.

A) Representative images of H&E staining in mouse lung sections (scale bar = 50 μm). B) The inflammatory score was graded in four random fields for each lung section at 200× magnification. C) Cell counts for macrophages, eosinophils, lymphocytes and neutrophils in BALF. n=8-10 mice per group. Data are mean ± SD. *p<0.05; **p<0.01; ***p<0.001. Abbreviations: H&E staining, hematoxylin-eosin staining; PAS staining, periodic acid-schiff staining; BALF, bronchoalveolar lavage fluid.

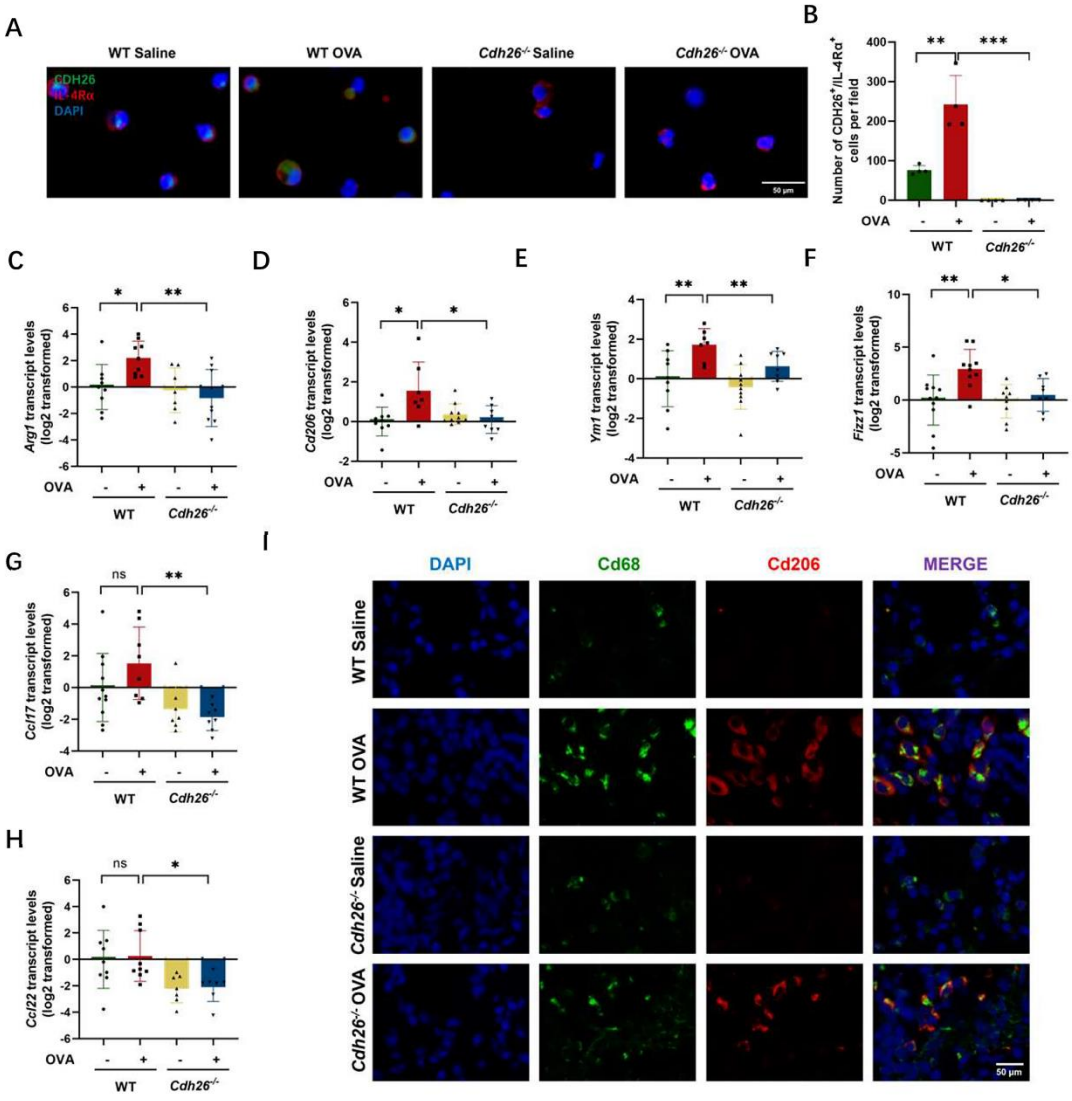

Figure E3 *Cdh26* deficiency suppresses the macrophage M2 polarization

A) Representative images for co-immunofluorescence staining of Cdh26 (green) and Il-4Rα (red) in BALF from mouse (scale bar = 50 μm). Nuclei was stained with DAPI (blue). B) The numbers of $Cdh26^{+}$/ $Il\text{-}4R\alpha^{+}$ cells in BALF were performed using ImageJ. C-H) The mRNA levels of *Arg1*, *Cd206*, *Fizz1*, *Ym1*, *Ccl22* and *Ccl17* in mouse lungs measured by quantitative PCR. The transcript levels were expressed as log2 transformed and relative to the mean value for control group. I) Representative images for co-immunofluorescence staining of Cd68 (green) and Cd206 (red) in BALF from

mouse (scale bar = 50 μm). n=8-10 mice per group. Data are mean ± SD. *p<0.05; **p<0.01; ***p<0.001. Abbreviations: Cd68, Cd68 molecule; Cd206, mannose receptor C-type 1; Arg1, arginase-1; YM1, also named as Chil3, chitinase-like protein 3; Fizz1, found in inflammatory zone 1; Ccl17, C-C motif chemokine ligand 17; Ccl22, C-C motif chemokine ligand 22; Il-4Rα, lnterleukin-4 receptor subunit alpha.

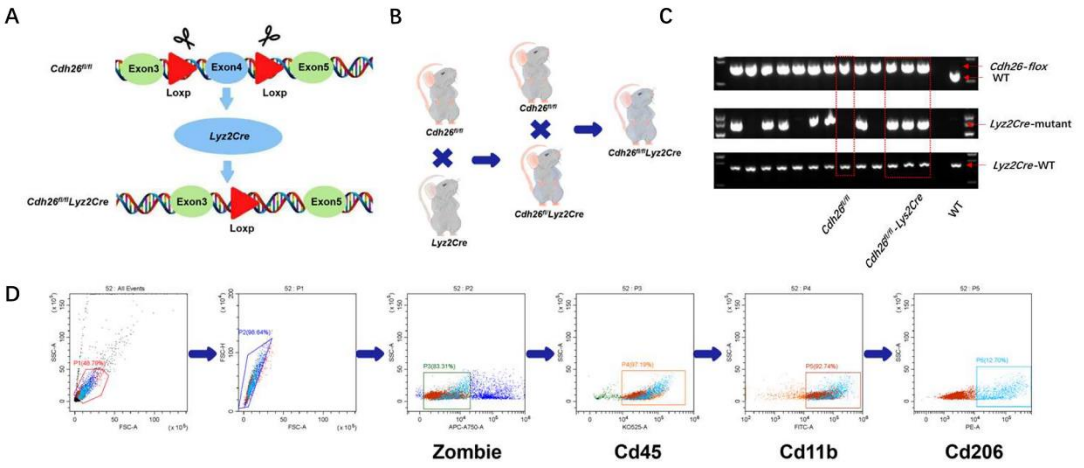

Figure E4 Construction strategies and breeding strategies for *Cdh26*$^{fl/fl}$ *Lyz2Cre* mice.

A) Construction strategies for *Cdh26*$^{fl/fl}$ *Lyz2Cre* mice. B) Breeding strategies for *Cdh26*$^{fl/fl}$ *Lyz2Cre* mice. C) Genetic identification *Cdh26*$^{fl/fl}$ *Lyz2Cre* mice. D) Gating strategies for flow cytometry. Abbreviations: Cd45, Cd45 antigen; Cd11b, Cd11 antigen-like family member b; Cd206, mannose receptor C-type 1.

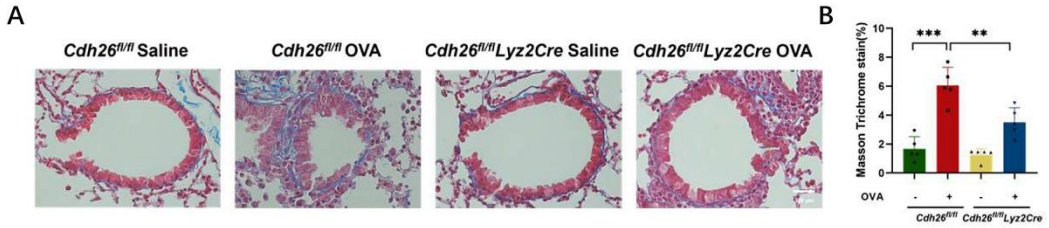

Figure E5 *Cdh26* deficiency inhibited airway remodeling.

A) Representative images of masson staining in mouse lung sections (scale bar = 50 μm). B) The area of masson trichrome stain were measured by ImageJ software. Data are mean ± SD. **p<0.01; ***p<0.001.

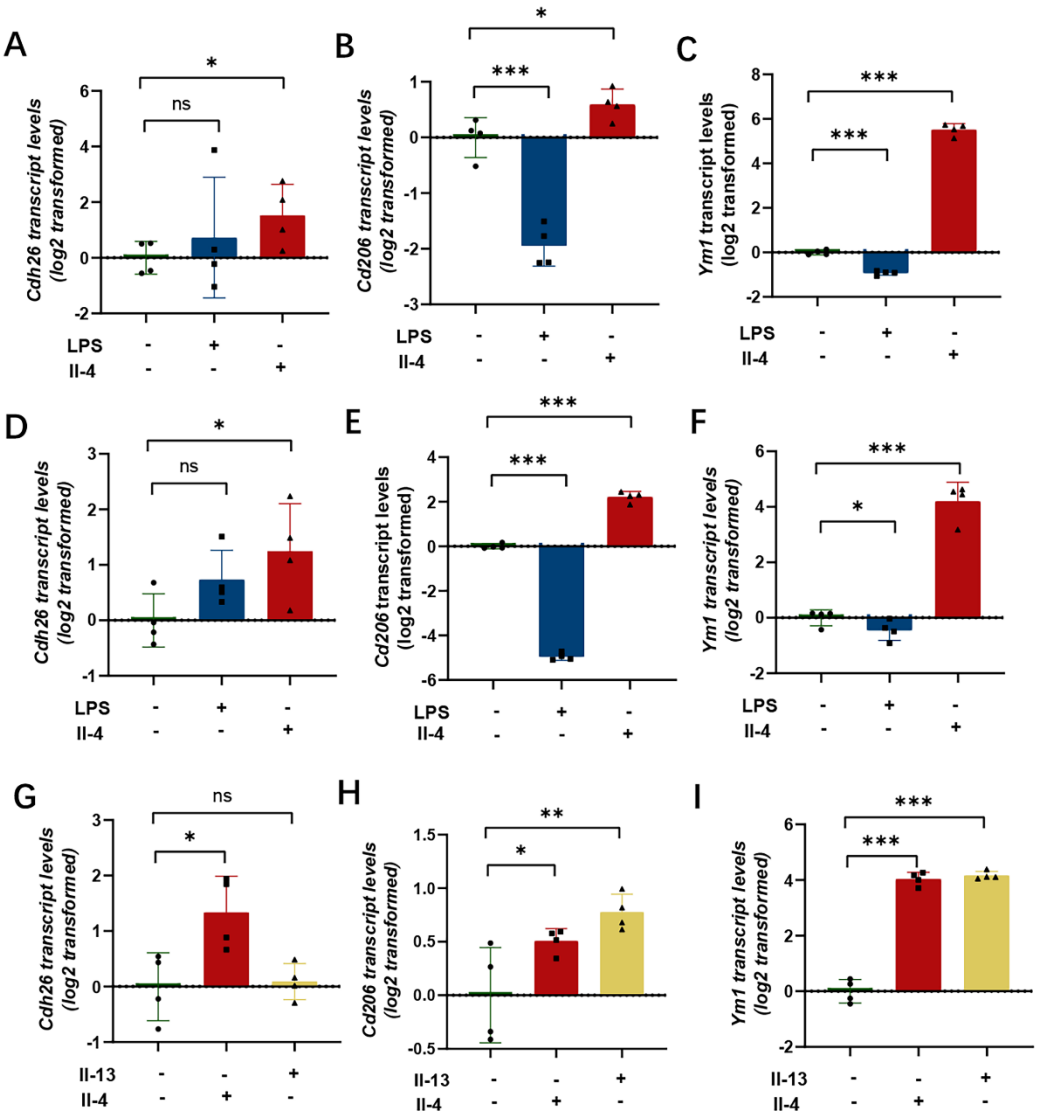

Figure E6 IL-4 induces increased expression of CDH26 in bone marrow-derived macrophages and mouse pulmonary macrophages.

A-C) Primary culture of BMDMs were stimulated with Il-4 or LPS for 48h. The mRNA levels of *Cdh26*, *Cd206* and *Ym1* were determined by quantitative PCR. D-E) Primary culture of mouse pulmonary macrophages were stimulated with Il-4 or LPS for 48h. The mRNA levels of *Cdh26*, *Cd206* and *Ym1* were determined by quantitative PCR. G-I) Primary culture of BMDMs were stimulated with Il-4 or Il-13 for 48h. The mRNA levels of *Cdh26*, *Cd206* and *Ym1* were determined by quantitative PCR. The transcript

levels were expressed as log2 transformed and relative to the mean value for control group. Data are mean ± SD. *p<0.05; **p<0.01; ***p<0.001. Abbreviations: Cdh26, cadherin-26; Cd206, mannose receptor C-type 1; YM1, also named as Chil3, chitinase-like protein 3; LPS, lipopolysaccharides.

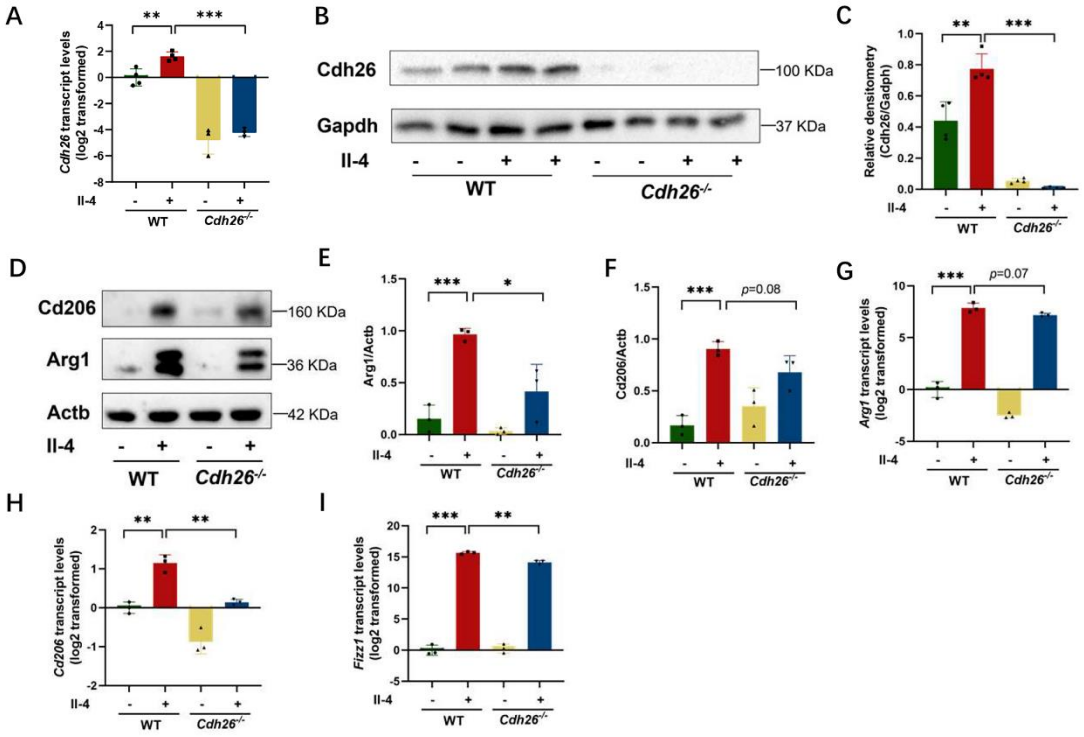

Figure E7 *Cdh26* deficiency suppresses M2 polarization of bone marrow-derived macrophages in vitro.

A) Primary culture of BMDM cells were stimulated with Il-4 for 48h. The mRNA levels of *Cdh26* were determined by quantitative PCR. The transcript levels were expressed as log2 transformed and relative to the mean value for control group. B-C) The protein levels of Cdh26 in BMDM cells after exposure to Il-4 for 48h were determined by western blotting. Densitometry assay was performed using ImageJ, and Cdh26 protein levels were indexed to Gapdh. D-F). The protein levels of Arg1, Cd206 in BMDM cells after exposure to Il-4 for 48h were determined by western blotting. Densitometry assay was performed using ImageJ, and Arg1, Cd206 protein levels were indexed to Actb. G-I) The mRNA levels of *Arg1*, *Cd206* and *Fizz1* were determined by quantitative PCR. The transcript levels were expressed as log2 transformed and relative to the mean value

for control group. Data are mean ± SD. *p<0.05; **p<0.01; ***p<0.001. Abbreviations: Cdh26, cadherin-26; BMDM, bone marrow derived macrophage; Cd206, mannose receptor C-type 1; Arg1, arginase-1; Fizz1, found in inflammatory zone 1; Actb, actin beta; Gapdh, glyceraldehyde-3-phosphate dehydrogenase.

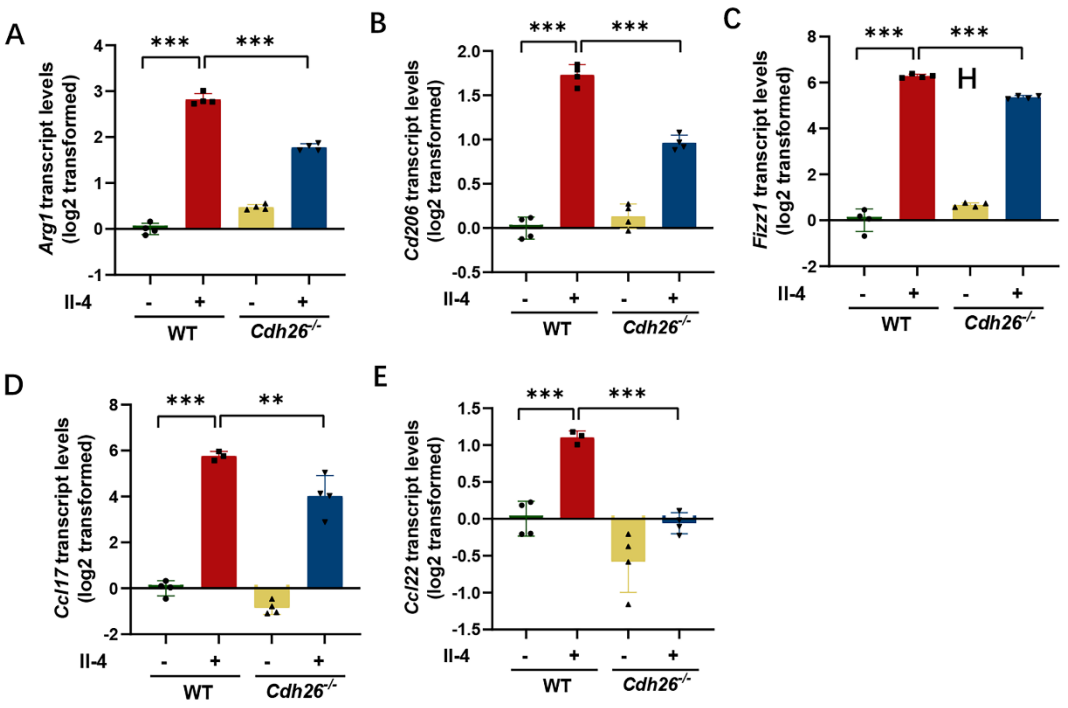

Figure E8 *Cdh26* deficiency suppresses M2 polarization of mouse pulmonary macrophages in vitro.

A-E) The mRNA levels of Arg1, Cd206 and Fizz1, Ccl17 and Ccl22 were determined by quantitative PCR. The transcript levels were expressed as log2 transformed and relative to the mean value for control group. Data are mean ± SD. *p<0.05; **p<0.01; ***p<0.001. Abbreviations: Arg1, arginase-1; Cd206, mannose receptor C-type 1; Fizz1, found in inflammatory zone 1; Ccl17, C-C motif chemokine ligand 17; Ccl22, C-C motif chemokine ligand 22, Actb, actin beta.

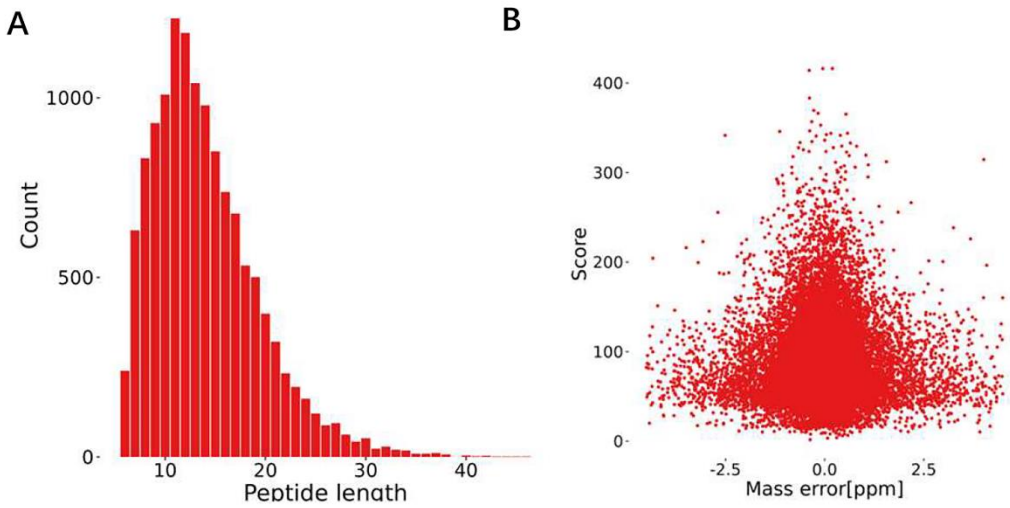

Figure E9 The quality control in mass spectrometry analysis.

A) The peptide length distribution of mass spectrometry analysis. B) The mass deviation distribution plot of mass spectrometry analysis.

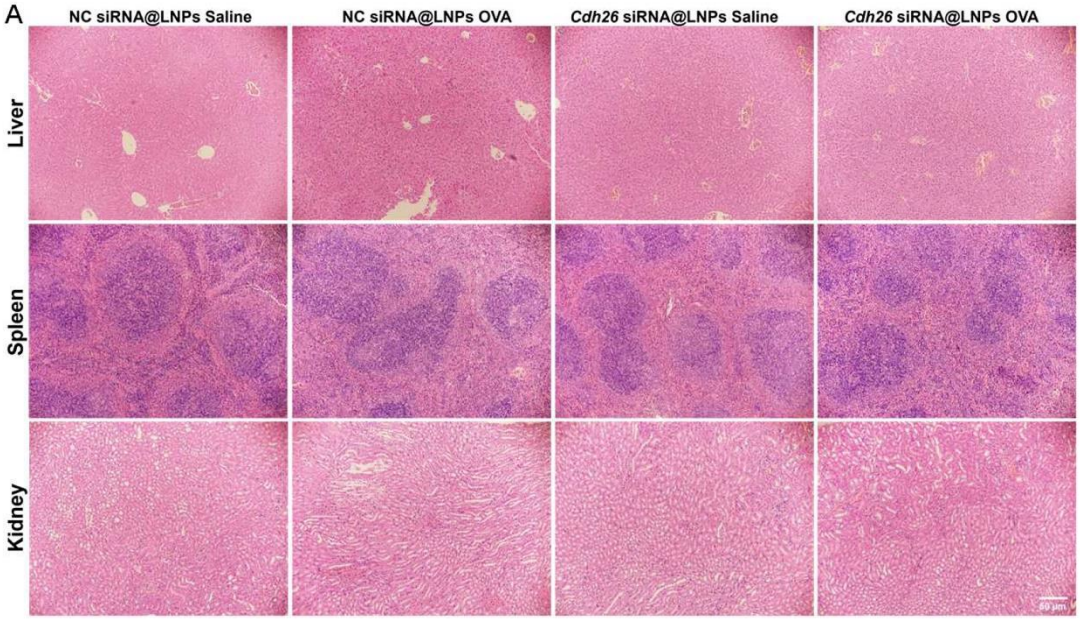

Figure E10 H&E staining images of major organs including liver spleen and kidney.

WT mice were treated with NC siRNA@LNPs + Saline, NC siRNA@LNPs + OVA, *Cdh26* siRNA@LNPs + Saline or *Cdh26* siRNA@LNPs + OVA, respectively. Representative images for H&E staining of major organs including liver spleen and kidney. n=8-10 mice per group.

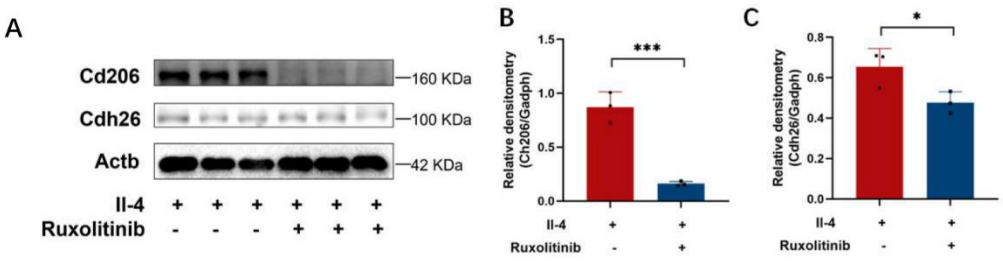

Figure E11 The JAK1 inhibitor ruxolitinib inhibits the expression of CDH26 in IL-4-induced bone marrow-derived macrophages.

A-C) Primary culture of BMDM cells were stimulated with Il-4 for 48h, and ruxolitinib was administered as an intervention 2 h ago. The protein levels of Cdh26, Cd206 were determined by western blotting. Densitometry assay was performed using ImageJ, and Cdh26, Cd206 protein levels were indexed to Gapdh. Data are mean ± SD. *p<0.05; ***p<0.001. Abbreviations: Cdh26, cadherin-26; Cd206, mannose receptor C-type 1; Actb, actin beta.

Table E1. Primers for quantitative PCR

Gene	Species		Primer sequence (5'-3')
GAPDH	Human	Forward	AAGGTGAAGGTCGGAGTCAAC
		Reverse	GGGGTCATTGATGGCAACAATA
CDH26	Human	Forward	CCTACCTCACGTCTACAGCGA
		Reverse	TTGAACCCAAAGAGTCCAGCA
CD206	Human	Forward	GGGTTGCTATCACTCTCTATGC
		Reverse	TTTCTTGTCTGTTGCCGTAGTT
FIZZ1	Human	Forward	AGCTCTCGTGTGCTAGTGTC
		Reverse	TGAACATCCCACGAACCACA
CCL17	Human	Forward	CTTCAAGGGAGCCATTCCCC
		Reverse	CTCTTGTTGTTGGGGTCCGA
IL4RA	Human	Forward	AAATCGTGAACTTTGTCTCCGT
		Reverse	CCCAGTGCCCTCTACTCTCAT
STUB1	Human	Forward	AGCAGGGCAATCGTCTGTTC
		Reverse	CAAGGCCCGGTTGGTGTAATA
Gapdh	Mouse	Forward	AGAGAGGCCCAGCTACTCG
		Reverse	CCAGCAGAAATCCTTCCAAGGAG
Actb	Mouse	Forward	CAGCCTTCCTTCTTGGGTATG
		Reverse	GGCATAGAGGTCTTTACGGATG
Cdh26	Mouse	Forward	GACAAGTGTCAGTTCCACGACAGC
		Reverse	TTCTCCATTTGGATGGAGGTGCTGG

Cd206	Mouse	Forward	CTCTGTTCAGCTATTGGACGC
		Reverse	TGGCACTCCCAAACATAATTTGA
Arg1	Mouse	Forward	TTGGGTGGATGCTCACACTG
		Reverse	GTACACGATGTCTTTGGCAGA
Ym1	Mouse	Forward	GCTCTTCATCTGTCAGCTTTGG
		Reverse	TGTGAGAGCAAGAAACAAGCAT
Fizz1	Mouse	Forward	TGGCTTTGCCTGTGGATCTT
		Reverse	CAGTGGTCCAGTCAACGAGT
Ccl24	Mouse	Forward	CAGCCTTCTAAAGGGGCCAA
		Reverse	GCTGGTCTGTCAAACCCCAA
Ccl17	Mouse	Forward	TACCATGAGGTCACTTCAGATGC
		Reverse	GCACTCTCGGCCTACATTGG
Ccl22	Mouse	Forward	CTCTGCCATCACGTTTAGTGAA
		Reverse	GACGGTTATCAAAACAACGCC
Stub1	Mouse	Forward	CCATCACTCGGAACCCACTTG
		Reverse	TGGCCTCATCATAACTCTCCA
Il4ra	Mouse	Forward	TGACCTCACAGGAACCCAGGC
		Reverse	GAACAGGCAAAACAACGGGAT

Table E2. The characterization of LNPs.

	Cdh26 siRNA-LNP	NC siRNA-LNP
concentration (mg/ml)	1.0±3%	1.0±3%
Encapsulation efficiency (%)	95.4	95.4
Particle size (nm)	86.21	84.72
Zeta potential (mV)	-0.74	-0.17
Polydispersity index	0.13	0.18

Reference

1. Barcellos VA, Dos Santos VCH, Moreira MÂ F, Dalcin PTR. Asthma control and sputum eosinophils in adult patients: a cross-sectional study in southern Brazil. *Scientific reports* 2023; 13: 21464.

2. Liang Y, Feng Y, Wu W, Chang C, Chen D, Chen S, Zhen G. microRNA-218-5p plays a protective role in eosinophilic airway inflammation via targeting δ-catenin, a novel catenin in asthma. *Clinical and experimental allergy : journal of the British Society for Allergy and Clinical Immunology* 2020; 50: 29-40.

3. Zhang K, Liang Y, Feng Y, Wu W, Zhang H, He J, Hu Q, Zhao J, Xu Y, Liu Z, Zhen G. Decreased epithelial and sputum miR-221-3p associates with airway eosinophilic inflammation and CXCL17 expression in asthma. *American journal of physiology Lung*

cellular and molecular physiology 2018; 315: L253-l264.